Defence Technology xxx (xxxx) xxx

Contents lists available at ScienceDirect

Defence Technology

journal homepage: www.keaipublishing.com/en/journals/defence-technology

A systematic review on advanced surface coating technologies for high-pressure piston pumps

Yifei Dong [a], Zhichao Jiao [a], Yangyang Ma [a], Qing Zhou [a,e,*], Ming Yang [a], Xing Ran [b,c,**], Zhe Wang [c], Chengjiang Tang [b], Yulong Li [d], Xiner Li [a], Haishan Teng [e], Xiaojiang Lu [e], Xuebo Liu [e]

[a] Research & Development Institute of Northwestern Polytechnical University in Shenzhen, Shenzhen, 518063, China
[b] AVIC Heavy Machinery Co. Ltd., Guiyang, 550005, China
[c] AVIC Heavy Machinery Research Institute, Guiyang, 550005, China
[d] Institute for Applied Materials (IAM), Karlsruhe Institute of Technology (KIT), Karlsruhe, 76131, Germany
[e] AVIC Liyuan Hydraulie Co, Ltd, Guiyang, 550018, China

ARTICLE INFO

Article history:
Received 27 May 2025
Received in revised form
25 August 2025
Accepted 24 October 2025
Available online xxx

Keywords:
Tribological performance
Advanced coatings
Piston pump
Multiple-principal element
Aeronautics applications

ABSTRACT

Piston pumps are extensively employed in the industrial and aerospace sectors, particularly in applications that demand high-pressure operation and precise flow regulation. However, the inherent structural complexity of these components, coupled with their frequent exposure to adverse operating conditions, leads to various forms of surface degradation in friction pair elements. To address these challenges, researchers have pursued the development of advanced coating technologies aimed at enhancing surface hardness, reducing friction coefficients, and improving wear resistance. These coatings typically include metallic coatings, ceramic coatings, and diamond-like carbon (DLC) coatings, along with more cutting-edge yet highly promising high-entropy alloy (HEA) coatings. As a novel class of materials, HEA coatings hold considerable potential to overcome the inherent limitations of conventional coating systems. This review provides a comprehensive overview of recent advances in piston pump coating technologies, with particular emphasis on deposition methodologies, microstructural characteristics, and tribological performance. By establishing microstructure-property relationships within these coating systems, this study proposes future research directions for optimizing surface engineering approaches in hydraulic pump applications.

1. Introduction

High-pressure piston pumps have been widely adopted across various industrial and aerospace sectors, attributed to their capability to handle high-pressure environments, deliver precise flow regulation, and support a wide variety of fluid types [1–3]. Typical applications include hydraulic systems for heavy machinery, aerospace systems for fuel and hydraulic operations, and industrial machinery for cooling and lubrication systems [4,5]. In aviation, where weight reduction critically impacts fuel efficiency, payload capacity, and mission range, enhancing pressure and speed significantly improves power-to-weight ratios [6]. However, this power-to-weight ratios optimization intensifies tribological challenges. Higher pressure increases the contact stress between friction pairs, while lightweight materials such as high-strength alloys typically exhibit poor tribological properties. These combined effects have raised the demand for reliable operation under extreme conditions, posing greater challenges to the manufacturing and performance of piston pumps.

As illustrated in Fig. 1(a), piston pumps comprise three critical friction pairs: the piston-cylinder interface, the valving plate assembly, and the slipper-swashplate conjunction. These tribological systems fulfill two essential functions during pump operation.

* Corresponding author. Research & Development Institute of Northwestern Polytechnical University in Shenzhen, Shenzhen, 518063, China.
** Corresponding author. AVIC Heavy Machinery Co. Ltd., Guiyang, 550005, China.
E-mail addresses: zhouqing@nwpu.edu.cn (Q. Zhou), ranxingavic@163.com (X. Ran).

Peer review under the responsibility of China Ordnance Society.

https://doi.org/10.1016/j.dt.2025.10.018

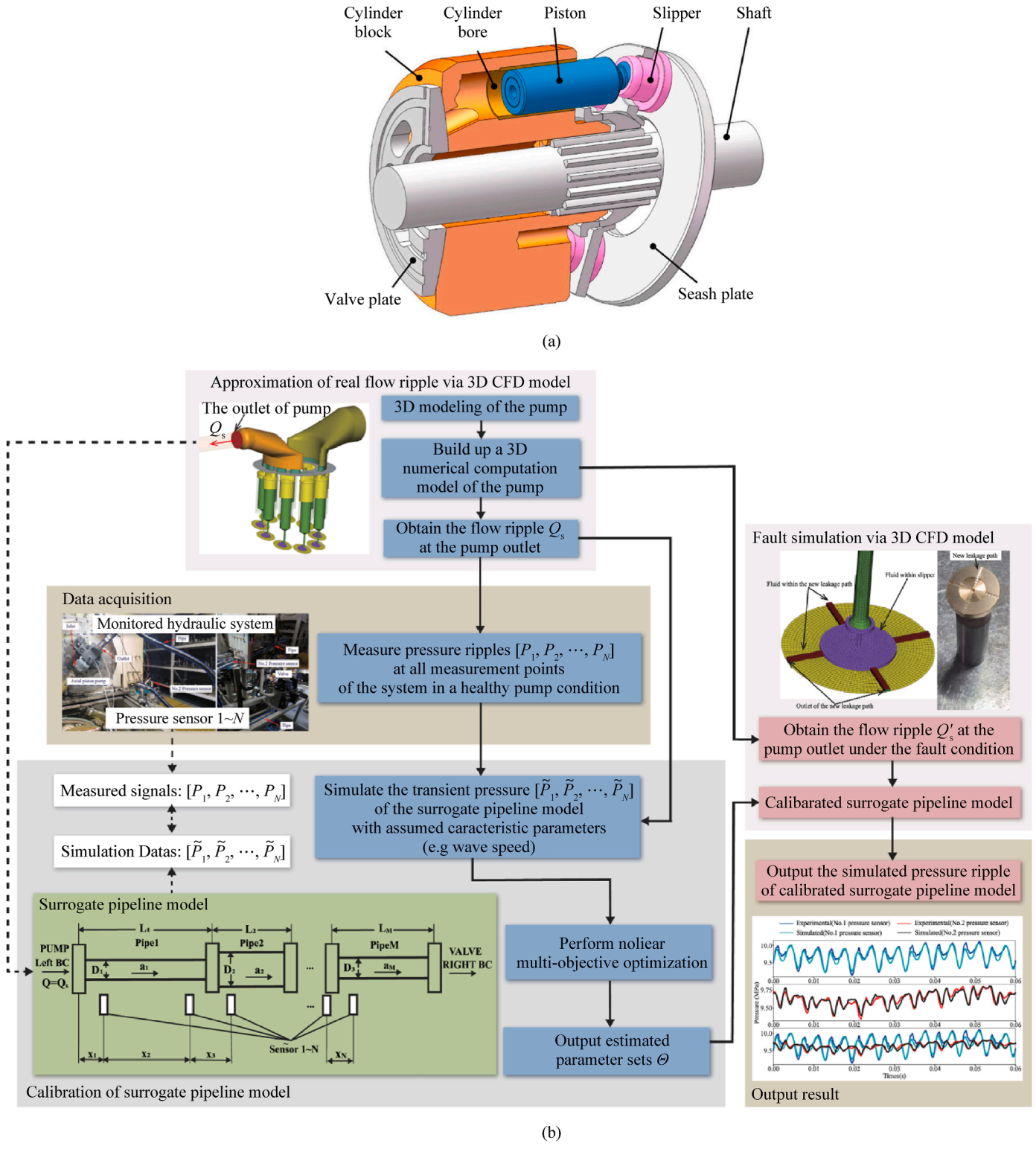

Fig. 1. (a) Working component of Axial Piston Pump [16]; (b) The flow chart of the proposed method for fault simulation of axial piston pumps [15].

Primarily, they establish pressure containment capability through precisely machined sealing surfaces between reciprocating components, preventing catastrophic leakage of high-pressure fluid that would compromise volumetric efficiency and pressure sustainability. Secondarily, they maintain hydrodynamic lubrication regimes to mitigate premature wear failure and thermal seizure [7–11]. Nevertheless, the pumps' structural complexity and exposure to severe operational challenges, including particulate contamination and thermal cycling, induce multifaceted surface degradation patterns across these critical interfaces [12–14]. Given that material wear predominantly initiates at surface layers, surface engineering through cost-effective coating deposition with

the help of fault simulation analysis (Fig. 1(b)) has become the predominant industrial approach for enhancing tribological performance while maintaining favorable cost-performance ratios [15].

Currently, there are several types of coatings applied to the components of piston pumps. DLC coatings are widely recognized for their exceptional wear resistance and low friction properties, making them particularly suitable for high-wear and high-pressure environments [17–19]. Ceramic coatings, characterized by their high strength and excellent corrosion resistance, are ideal for applications involving corrosive fluids [20–22]. Metal coatings are typically employed in scenarios that require high thermal conductivity and superior mechanical performance [23–25]. These coatings not only safeguard the surface from mechanical and chemical degradation but also provide effective lubrication, thereby reducing energy loss and improving operational efficiency. Among them, high-entropy alloy (HEA) coatings provide superior mechanical strength, corrosion resistance, thermal stability, and radiation tolerance through synergistic multi-element interactions [26–28]. Making them a highly competitive alternative to traditional coatings. Especially outstanding in reducing wear rate, compared with traditional coatings, its wear rate can be significantly reduced by 30%–50% [29–31]. The following systems compare the comprehensive performance of four types of coatings (Table 1).

Past reviews of coatings systematically organized the preparation techniques, performance advantages, and application scenarios of various coating materials. Their core advantage lies in providing a comparative framework across materials and processes, closely following industrial needs, and tracking cutting-edge trends, providing a clear network and reference for research and development [32–34]. However, existing literature exhibits two critical. Firstly, there is a lack of systematic integration of key findings to guide the microstructure optimization of axial piston pump coatings, resulting in a vague understanding of the microstructure performance relationship of coating systems, which restricts the lubrication behavior and tribological performance improvement of high-pressure axial piston pumps; Secondly, the updating of emerging technologies and materials lags behind, impeding comprehensive understanding of recent advancements. Addressing these gaps is crucial for improving the tribological performance of next-generation coating materials and the reliability of high-pressure piston pumps.

This study undertakes a comprehensive review of recent advancements in piston pump coating technologies, specifically examining the preparation processes, microstructural compositions, and tribological characteristics of metals, ceramics, DLC coatings, and other advanced coatings. Building on recent literature findings, this paper systematically compares HEA coatings with traditional coatings for piston pumps for the first time, and systematically explores the relationship between the microstructure and properties of surface coatings. This review is organized as follows: Section 2 systematically reviews recent advancements in the processing techniques and microstructural characteristics of metallic, ceramic, DLC, and HEA coating systems. Section 3 conducts comprehensive evaluations of tribological performance metrics across these four coating categories. Building upon established research foundations, Section 4 assesses prevailing technical challenges and proposes strategic development pathways. By implementing systematic benchmarking analysis of coating functional parameters, the review aims to provide valuable insight for both academic investigators and engineering practitioners.

2. Preparation and microstructure of coating for key friction pairs

The microstructural and performance attributes of piston pump coatings—such as grain size, phase composition, porosity, and interfacial bonding—are predominantly dictated by the preparation technology. Key methodologies include physical vapor deposition (PVD) employing magnetron sputtering or thermal evaporation techniques to fabricate dense coatings with low-thermal-impact characteristics, particularly suitable for precision components [35,36]; Chemical vapor deposition (CVD) employing controlled gas-phase reactions of metal-organic precursors to synthesize wear-resistant ceramic-metallic architectures, demonstrating exceptional high-temperature stability [37,38]; Cold spraying can minimize thermal exposure, preserve the original microstructure such as temperature sensitive phases and nanocrystals, and effectively prevent thermal deformation or degradation of the substrate [39,40]. Advanced thermal spraying variants including atmospheric plasma and high-velocity oxy-fuel (HVOF) techniques that propel molten feedstock materials to create thick, metallurgically bonded deposits for heavy-duty applications [41,42]; Electrochemical deposition processes that generate metallic coatings with tailored ductility and moderate hardness through optimized reduction reactions, primarily employed for corrosion protection [43–45]. The optimal selection of coating technologies is achieved by tailoring the microstructure in accordance with substrate compatibility, operational demands (e.g., thermal stability, wear resistance), and cost-effectiveness, thereby ensuring superior performance. The following will detail the specific types of coating preparation technologies (Table 2).

2.1. Metal coating

The metal coating technology originated from the beeswax resin coating on ancient Egyptian bronze ware, and the modern system began with the epoxy coal tar coating developed by Hoffman in 1870. In the 20th century, driven by the demands of war and aviation, electroplating technology developed hard chromium and copper alloy processes and automated production lines, and hot-dip plating significantly improved corrosion resistance [46]. Currently, materials science and nanotechnology are driving innovation in high-performance coatings. Cold spraying achieves

Table 1
Comprehensive performance of coatings.

Performance Index	Metal coating	Ceramic coating	DLC coating	HEA coating
Hardness/GPa	0.4–15	15–35	20–50	14–20
Coefficient of Friction (COF)	0.4–0.8	0.2–0.6	0.05–0.2	0.3–0.7
Maximum Operating Temperature/°C	300–600	800–1,600	300–450	500–800
Corrosion Eesistance	Limited	Excellent	Excellent	Excellent
Toughness	Excellent	Poor	Limited	Limited
Conductivity	Excellent	Poor	Limited	Limited
Main applications	Buildings; bridges;	Aviation engine	Precision cutting tool	Aviation bearings

Table 2
Coating preparation technologies.

Technology	Advantages	Disadvantages	Application Fields
Physical Vapor Deposition (PVD)	Precise control of film thickness and composition; Dense nanostructures with strong adhesion	Limited thickness; High equipment cost; Low efficiency of large-scale sedimentation	Wear resistant coating for key friction pairs of piston pumps
Chemical Vapor Deposition (CVD)	High deposition rate; Superior high-temp stability; Strong adhesion strength	Substrate thermal degradation; Toxic precursors	Semiconductor and Integrated Circuit Manufacturing
Cold Spray Technology	No thermal damage; High coating density; High deposition rate	High equipment requirements; limited to spraying soft metal materials;	Thermal sensitive components in the aerospace field
Thermal Spray Technology	Prepare thick coatings; Suitable for large area components; High adhesion strength	High porosity; Possible introduction of oxidation	Engine components; Construction machinery
Electrochemical Deposition	Simple process; Low cost; Adjustable coating ductility and hardness	High porosity; High porosity; Environmental concerns	Semiconductor and Integrated Circuit Manufacturing

strengthening of magnesium lithium alloy substrates, and multi-layer electroplated aluminum bronze enhances wear resistance through gradient design [47]; HVOF spray particle reinforced bronze coating enhances hardness [48]. These technologies are widely used in key friction pairs such as plunger pumps, solving high-pressure wear problems through self-lubricating behavior and phase change strengthening, meeting the needs of aerospace lightweighting, automotive corrosion and wear resistance, and energy equipment resistance to extreme environments.

Metal coatings exhibit critical tribological significance due to their exceptional fracture toughness, wear resistance, and multi-functional protective capabilities [49,50]. These coatings enhance mechanical durability through self-lubricating behavior that reduces friction coefficient and operational reliance on external lubricants, particularly under extreme conditions [51]. The synergistic characteristics of mechanical strengthening, environmental adaptability, and energy efficiency make metal coatings an indispensable solution to the challenges of modern industrial tribology.

The precise kinematic control of machine components necessitates engineered surfaces with optimized roughness, stringent dimensional tolerances, and superior tribological performance. Specifically controlled frictional behavior and enhanced wear resistance to mitigate material loss under cyclic contact stresses. Das et al. [52] synthesized diamond-reinforced nanostructured bronze coatings via high-energy ball milling and HVOF thermal spraying, achieving 150–200 μm thick coatings. The composite coating exhibited a lamellar microstructure with dispersed diamond-rich regions (dark phases), while the pure bronze coating displayed Cu or Sn phase segregation due to melting point disparities, confirmed by EDS (Energy Dispersive X-ray Spectroscopy) analysis (Fig. 2). The HVOF process preserved diamond's sp^3 hybridization by minimizing thermal exposure through rapid particle acceleration and short flame interaction, while the molten bronze matrix prevented diamond oxidation. This methodology significantly enhanced coating hardness and wear resistance, demonstrating effective diamond dispersion and structural protection, critical for tribological applications.

Cold spraying technology, as an advanced coating preparation method, can provide protection to the surface of magnesium-lithium alloys without destroying the properties of the substrate. This advanced solid-state particle deposition approach enables effective surface enhancement without compromising the structural integrity of the lightweight alloy system. Wan et al. [47] demonstrated that cold-sprayed aluminum bronze coatings on MBLS10A-200 Mg-Li alloys achieved exceptional interfacial bonding. The coating exhibited superior densification (1.56% porosity) with characteristic jagged interfacial morphology (Fig. 3), where mechanical interlocking between deformed particles and substrate-induced material jetting was observed. Controlled deposition experiments revealed that high-velocity particle impacts generated adiabatic shear instability at particle or substrate interfaces, initiating localized plastic strain and thermal softening effects. This dynamic process effectively removed surface oxides through intense shear deformation, enabling simultaneous mechanical anchoring and elemental interdiffusion at clean metallic interfaces. The resultant hybrid bonding mechanism, combining mechanical interlocking with limited interfacial intermetallic formation, underscores cold spraying's unique capability for oxide-sensitive Mg-Li alloy surface enhancement without inducing detrimental thermal degradation.

HVOF has higher density and can distribute reinforcing phases layer by layer through melt flow, significantly improving wear resistance. But its high temperature process may cause thermal damage to the substrate. Cold spraying avoids thermal effects and protects heat sensitive substrates through solid-state deposition. But its coating porosity is slightly higher, and the reinforcing phase is dispersed in a spherical shape, lacking mechanical interlocking and limited improvement in wear resistance. Therefore, HVOF is more suitable for scenarios that require high density, optimized enhanced phase distribution, and substrate heat resistance, while cold spraying has more advantages in protecting heat sensitive substrates and avoiding thermal damage.

Electrodeposited aluminum bronze coatings have been widely applied in piston pumps due to their excellent combination of mechanical wear resistance and corrosion protection. Liang [53] engineered a functionally graded aluminum bronze coating (> 20 μm) on QAL10-4-4 substrates via hollow cathode discharge (HCD) ion plating, employing layer-by-layer deposition (3–4 μm/layer) to achieve a microstructural transition from substrate-proximal equiaxed grains to columnar morphology in upper strata. Compositional profiling revealed progressive enrichment of Cu, Ni, Fe, and Al with increasing distance from the interface, culminating in dominant NiAl or CuAl intermetallic phases at the surface. Research has shown that this architectured design exhibits synergistic effects—such as multilayer-induced crack deflection and intermetallic phase hardening—that can significantly enhance microhardness and wear resistance. Electrodeposition, as an economical and scalable metal coating technology, allows for precise control of coating thickness and composition through process optimization, making it suitable for mass production of complex components [54]. However, due to slow sedimentation rate, low efficiency of thick coatings, and insufficient adaptability to extreme working conditions, practical applications need to balance cost and performance requirements.

2.2. Ceramic coating

The development of ceramic coatings began with the urgent need for material protection in extreme environments. In the early days, the insufficient performance of metal materials under high temperature, corrosion, and high wear conditions promoted the

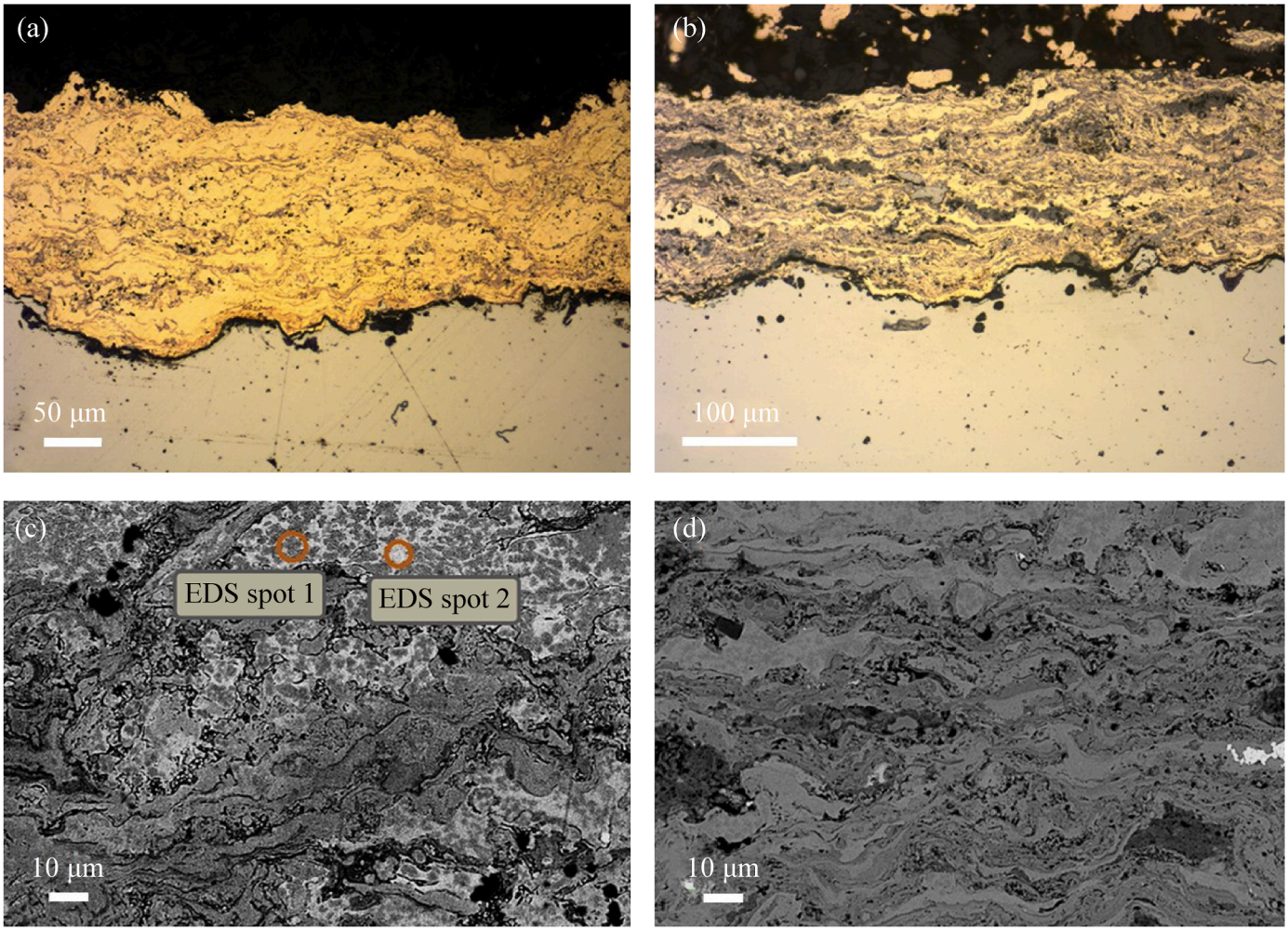

Fig. 2. (a) Optical micrographs of pure bronze coating; (b) Diamond reinforced composite coating; (c) Back scattered electron images of pure bronze coating deposited from as-received bronze powder; (d) Composite bronze coating deposited using diamond reinforced ball milled powder feedstock [52].

exploration of ceramic coating technology. In the mid-20th century, the maturity of thermal spraying technologies such as plasma spraying enabled their industrial application, initially used in high-temperature and anti-oxidation scenarios. With the increasing demand for high hardness and low friction coatings in aerospace, hydraulic machinery and other fields, nitride ceramic coatings such as TiN and TiCN are precisely prepared through PVD and CVD technologies, solving the problems of weak adhesion and poor uniformity of traditional coatings [55,56]. In recent years, in order to cope with complex service conditions, composite ceramic coatings and gradient functional design have become research focuses. By regulating nanostructures and optimizing interfaces, balancing hardness and toughness, the inherent defects of ceramic materials such as high brittleness and easy cracking due to thermal mismatch have been gradually overcome, and their applications in key friction pairs, such as high-pressure piston pumps have been expanded [57,58].

Cermet composite coatings exhibit superior tribological performance in extreme operating conditions through synergistic ceramic-metal phase interactions, demonstrating exceptional wear resistance and high-temperature stability via oxide dispersion strengthening mechanisms [59–61]. Their engineered architectures, incorporating optimized carbide grain sizes and solid lubricant phases, implement a friction adaptation function [62]. In hydraulic system applications like axial piston pumps, these coatings mitigate adhesive wear through surface energy modification while providing electrochemical protection in corrosive media [63]. By engineering microstructural architectures spanning homogeneous single-phase systems to advanced composite and gradient configurations, these coatings achieve enhanced tribological performance through optimized stress distribution and interfacial compatibility [64].

Titanium-based ceramic coatings, such as TiN, TiCN, and TiAlN, demonstrate exceptional hardness and wear resistance, with their optimized mechanical and tribological properties significantly enhancing the operational durability of piston pumps [65–67]. Sui [68] engineered TiN/Ti_3AlN-Ti_3Al composite coatings on TC21 titanium alloy via laser cladding, establishing a critical specific energy threshold (58.3 J/mm^2) that governs coating integrity through melt pool dynamics. Cross-sectional analysis (Fig. 4) revealed morphological transitions from discontinuous melt pools with 12.7% porosity at 40.0 J/mm^2 to fully dense convex geometries at optimal energy, followed by crack propagation at excessive energies (> 58.3 J/mm^2) due to thermal stress accumulation. The parabolic dilution rate profile (3.5%–29.6%) demonstrated energy-dependent interfacial metallurgy, with 14.0% dilution at 58.3 J/mm^2 achieving synergistic benefits: sufficient Ti-Al interdiffusion for chemical bonding while maintaining coating or substrate

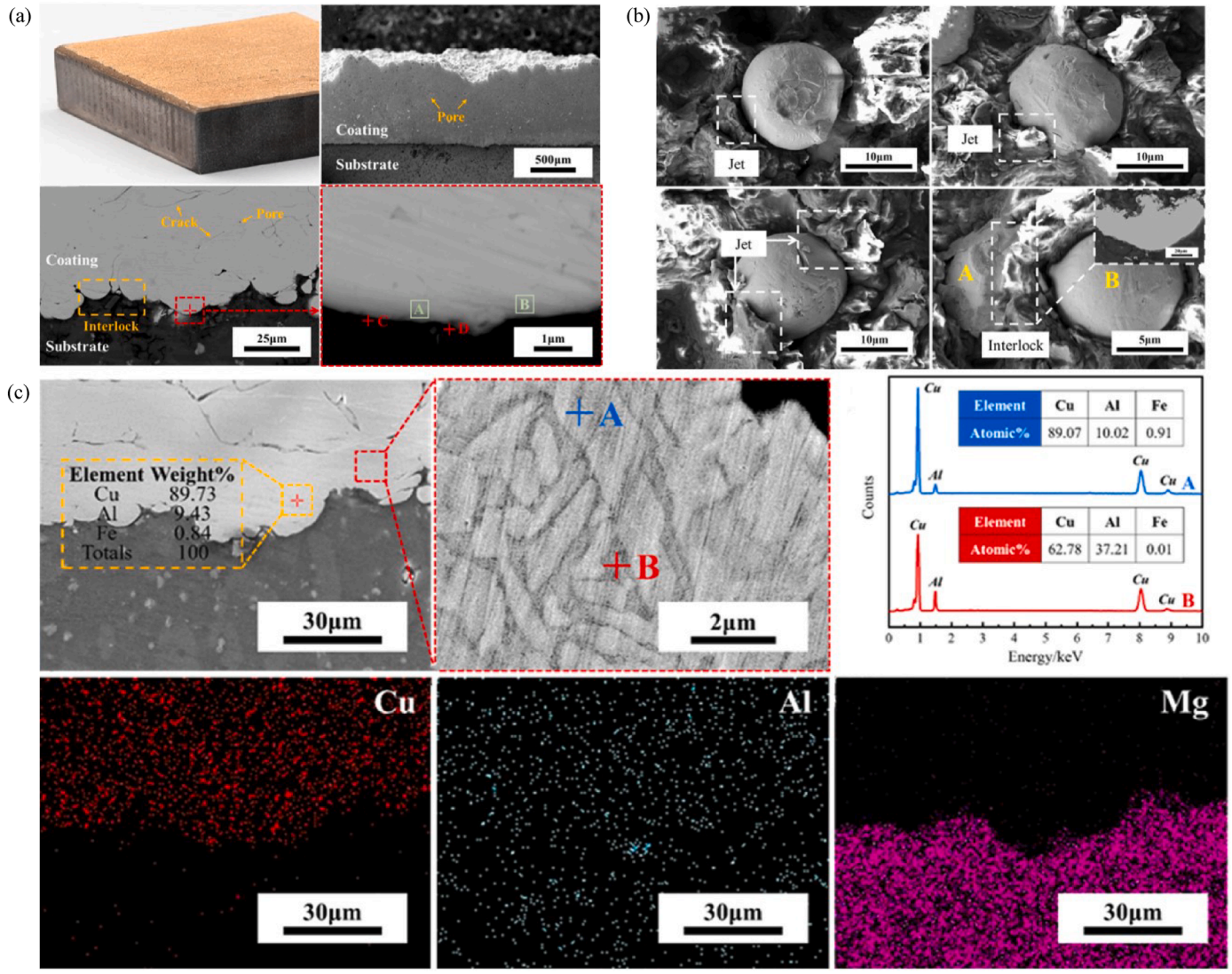

Fig. 3. (a) The macro morphology and microstructures of aluminum bronze coating; (b) SEM micrographs of the first layer build up of particles jet-type morphologies around the particle impact zone and the morphology of interlocking phenomena between sprayed particles; (c) SEM micrographs and EDS of aluminum bronze coating [47].

hardness differential. Mechanistic analysis identified dual failure modes - gas entrapment from low-energy solidification kinetics versus turbulent splashing-induced defects at high energy inputs. By combining the elimination of pores and Ti_3AlN dispersion strengthening, the wear life of the coating is significantly extended. This energy-microstructure-property correlation framework advances damage-tolerant coating design for piston pump surface hardening and fatigue resistance.

Interface engineering is crucial in optimizing coating performance, which synergistically improves the wear resistance and toughness of piston pump friction pairs through periodic layered structure deflection cracks, composition gradient optimization of residual stress, and nano layer interface blocking dislocations [69–72]. Konstantiniuk [73] investigated the grain boundary evolution mechanism in CVD deposited TiN/TiCN coatings under isothermal vacuum annealing, revealing critical microstructure-property relationships through cross-sectional scanning electron microscope (SEM) analysis (Fig. 5(a)). Both as-deposited and annealed coatings maintained characteristic V-shaped columnar TiCN grains with competitive growth textures, while EDS identified progressive W and Co segregation at TiN and TiCN interfaces, diffusion increasing with extended annealing duration. This intergranular diffusion induced grain boundary embrittlement, evidenced reduction in fracture stress despite unchanged macro-mechanical properties. These findings establish an optimization window for hardmetal TiN/TiCN/Al_2O_3 multilayer systems, suggesting controlled annealing durations to balance interfacial adhesion enhancement through limited diffusion against embrittlement risks, particularly crucial for piston pump coating applications requiring simultaneous fracture toughness and chemical stability.

Hard coatings are widely used in industrial applications to improve the performance and lifespan of piston pumps. The design of nanocomposite structures and nano-multilayer films can significantly improve the hardness, toughness, and wear resistance of coatings [74,75]. CrSiN/TiAlN multilayer coatings have attracted attention due to their high hardness and excellent oxidation resistance. Wu [76] engineered nanolaminated CrSiN/TiAlN coatings via bipolar asymmetric pulsed-DC magnetron sputtering, demonstrating that bilayer periodicity and

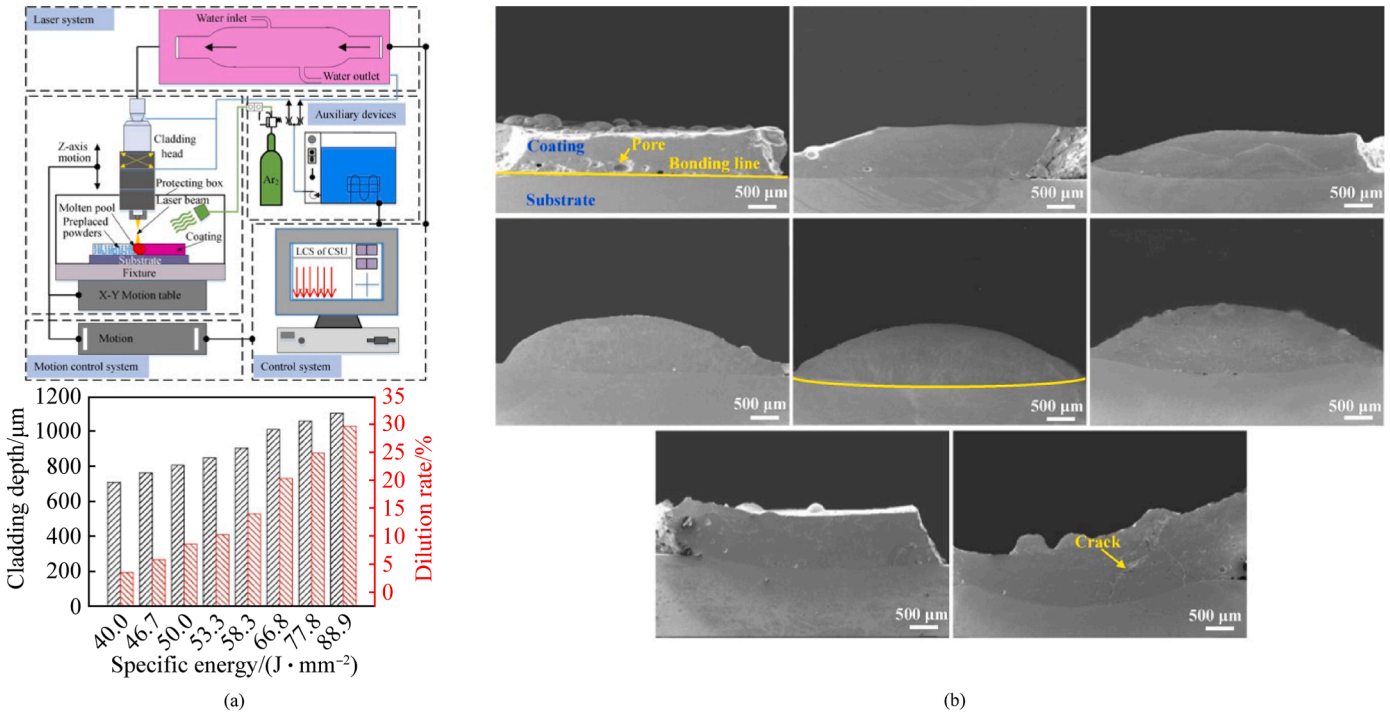

Fig. 4. (a) Schematic diagram of the laser cladding system; (b) Morphology of TiN/Ti_3AlN-Ti_3Al coatings at different specific energies [68].

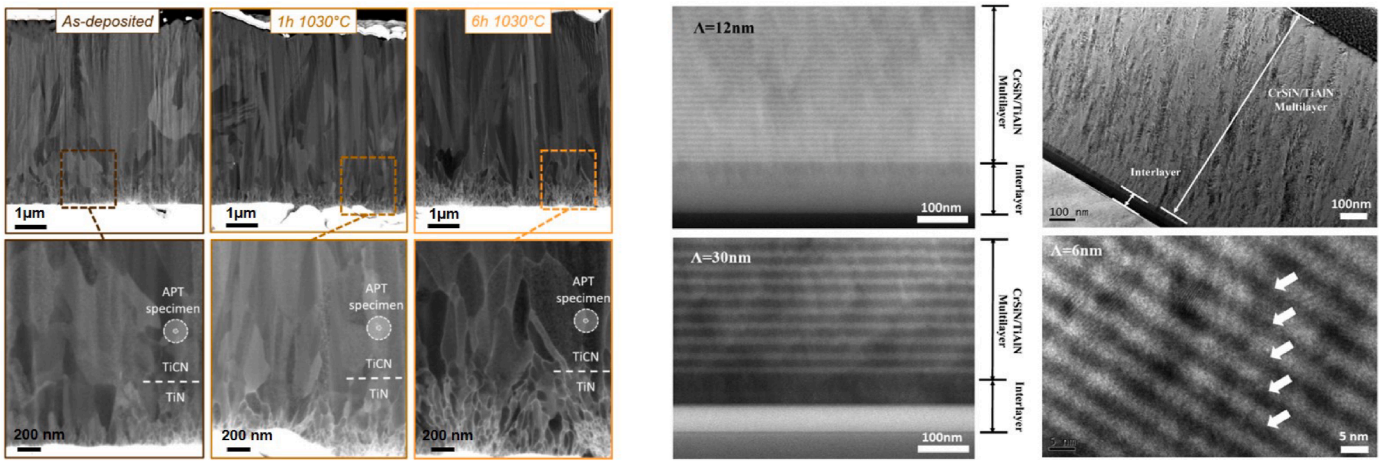

Fig. 5. (a) Cross-sectional SEM images of TiN/TiCN coatings [73]; (b) Cross-sectional SEM and TEM images of CrSiN/TiAlN multilayer coatings [76].

stoichiometric gradient govern mechanical performance through interfacial nanostructure design. Cross-sectional characterization (Fig. 5(b)) revealed dependent architectural evolution: 12 nm periods formed nanolaminates with textured columnar grains, while thicker layers developed discontinuous interfaces. The hardness extremum (31 GPa at 10 nm) originated from synergistic Hall-Petch strengthening and interfacial coherency strain, which caused hardness degradation due to interfacial intermixing. Compositional gradient optimization enhanced fracture toughness through residual stress modulation and nanolaminate-induced crack deflection. The study establishes a multilayer design paradigm where precisely controlled interfacial nanostructures enable hardness-toughness synergy.

2.3. Diamond-like carbon

The development of DLC coatings began in the 1970s, aimed at addressing the performance deficiencies of traditional materials in high-pressure and high wear environments. In the early stages, due to difficulties in regulating hydrogen content and sp^3 bonds, there were high internal stresses and weak binding forces [77]. At the end of the 20th century, the maturity of deposition technologies such as PVD and CVD achieved controllable preparation of soft and hard materials, solving the problems of uniformity and thermal stability defects. In recent years, the high-temperature stability, wear resistance, and bonding strength of coatings have been

significantly improved through element doping and gradient interface design, making them a key surface strengthening technology for high-pressure plunger pumps and other equipment [78,79].

Depending on the hydrogen content and sp^3 bond ratio, DLC can be categorized into two main types, soft (high H content) and hard (predominant sp^3 bonding) coatings. [80–82]. Hydrogenated soft coatings (a-C:H) with > 5 μm thickness for soft substrate protection through enhanced load-bearing capacity, and hydrogen-free hard variants dominated by sp^3 covalent bonds delivering extreme hardness and ultralow friction. Hydrogenated DLC achieves high toughness and low stress characteristics with high hydrogen content and an amorphous carbon network, but has poor thermal stability (degradation caused by hydrogen escape) and limited corrosion resistance. Hydrogen free DLC forms a dense structure with high sp^3 bonds, possessing both ultra-high hardness and heat resistance. However, due to high internal stress and columnar grain boundaries, it is prone to oxidation cracking in high-temperature and wet corrosion environments.

The archetypal tetrahedral amorphous carbon (ta-C), with > 70% sp^3 hybridization, demonstrates exceptional mechanical robustness (> 50 GPa hardness), thermal stability (> 400 °C), and tribochemical adaptability through in situ formation of 2–5 nm passivation layers during sliding [83–87]. Structural engineering dictates the application specificity of super-nano crystalline films (50–500 nm) to enable pump seal applications through nanoscale conformality [88]. However, performance degradation remains a challenge under high-temperature operating conditions (> 500 °C), primarily due to oxidative destabilization and columnar grain boundary cracking under high stresses. Amorphous ta-C, while avoiding grain boundary defects, still faces the limitation of reduced wear resistance at elevated temperatures [89]. Advanced deposition techniques like plasma-enhanced CVD and filtered cathodic arc (FCVA) enable defect-engineered diamond and ta-C coatings with tailored sp^3 hybridization through high ionization efficiency and interfacial energy modulation. Erdemir et al. [90] demonstrated that the tribological properties of diamond and ta-C coatings are intricately influenced by environmental factors. Humidity, temperature, and atmosphere regulate the frictional chemical reaction pathways, which can induce variations in the wear rate spanning up to two orders of magnitude.

AISI 4130 alloy steel is widely used in aerospace, piston pumps, and defense industries, but its insufficient surface hardness and wear resistance limit its application in harsh environments. W-doped hydrogenated diamond-like carbon coating, as a solid lubricant, has a low friction coefficient and high wear resistance, which can significantly improve the surface properties of the material. Efeoglu [91] fabricated tungsten-doped amorphous carbon (W-a:C-H) coatings on AISI 4130 steel via closed-field unbalanced magnetron sputtering (CFUBMS), employing Taguchi L9 orthogonal design to optimize critical parameters (C_2H_2 flow rate, W target current, pulse frequency, duty cycle). Pulsed DC plasma implementation suppressed arc discharges and enhanced plasma energy density, yielding dense, homogeneous ~1 μm-thick coatings with < 5% thickness variation across nine experimental groups (Fig. 6). Coating thickness exhibited a strong positive correlation with C_2H_2 flow rate (maximized at 18 sccm), driven by hydrocarbon dissociation-dominated deposition over low-efficiency carbon sputtering. ANOVA confirmed C_2H_2 flow rate as the dominant thickness control parameter, though excessive flow (> 20 sccm) induced hardness degradation.

Wang [92] synthesized hydrogenated amorphous carbon (a-C:H) films via high-frequency unipolar pulsed PECVD, systematically investigating bias voltage effects (−800 to −1,600 V) on microstructure and property. Elevated bias voltages promoted the

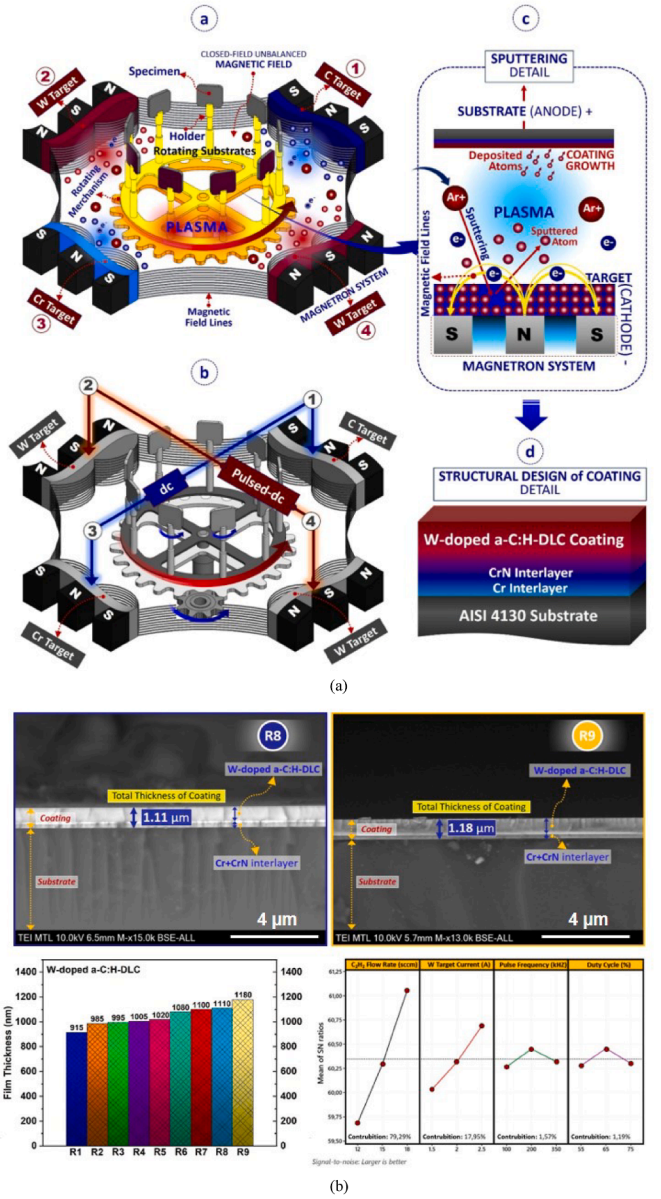

Fig. 6. (a) The target magnetron and the power supplies configuration of the CFUBMS deposition system and detail; (b) Typical cross-sectional SEM images of W-doped a-C:H-DLC coatings [91].

nucleation and growth of graphite within the amorphous matrix, as evidenced by HRTEM, with domain density increasing and lateral dimensions expanding at −1,600 V. This microstructural evolution enhanced chemical inertness while inducing a hardness and elasticity tradeoff: hardness decreased from 14.72 to 12.89 GPa, yet elastic recovery improved from 82.2% to 88.1%, demonstrating retained mechanical resilience. Tribologically, optimized graphitic domains reduced friction coefficients by 49% and wear rates by 34%, attributed to the in-situ formation of shear-induced graphitic tribofilms. The study establishes bias voltage as a critical lever for tuning structure, providing a plasma-engineering pathway to balance hardness and lubricity in protective coatings for piston pumps.

Zur [93] fabricated DLC coatings on Acrylnitril-Butadien-Styrol-Copolymer (ABS polymer) substrates via pulsed vacuum arc deposition (PVM-D), employing rotational substrate kinematics

and cathode pulse modulation to engineer coating architecture. Cross-sectional SEM revealed 1–5 μm-scale linear inhomogeneities correlated with pulsed arc-induced localized carbon supersaturation, while Atomic Force Microscopy (AFM) quantification demonstrated controlled surface roughness evolution through melt-reshaping mechanisms at plasma hotspots. This strategic non-uniformity generated a higher specific surface area through fractal-like carbon consolidation patterns, despite ABS's low thermal conductivity inducing transient thermal gradients during deposition. The Cr and In interlayer architecture (Fig. 7) effectively buffered interfacial stresses, maintaining coating adhesion despite thermomechanical mismatch. This work establishes pulsed arc parameter-space engineering as a viable route for tailoring DLC tribo-active surfaces on thermally sensitive polymers.

2.4. High-entropy alloy (HEA) coatings

The development of high entropy alloy coatings stems from breakthroughs in the performance limitations of traditional coatings. After the concept of high entropy alloys was proposed in 2004, the high hardness, corrosion resistance, and high-temperature stability brought by their multi principal component design have attracted much attention [94]. High entropy alloy coatings are prone to phase decomposition or segregation during preparation and service due to element diffusion and temperature fluctuations, leading to structural performance degradation. At the same time, it is difficult to achieve high uniformity, high efficiency, and low-cost deposition of large components. Therefore, it is necessary to suppress the precipitation of brittle phases through component gradient design to ensure stability. And with the help of multi-target collaborative sputtering, magnetic field optimization, and zone temperature control, the uniformity and efficiency of large-area deposition are improved. The demand for wear-resistant and corrosion-resistant coatings under extreme working conditions in aerospace and other fields has driven them to become an emerging solution for surface strengthening of high-

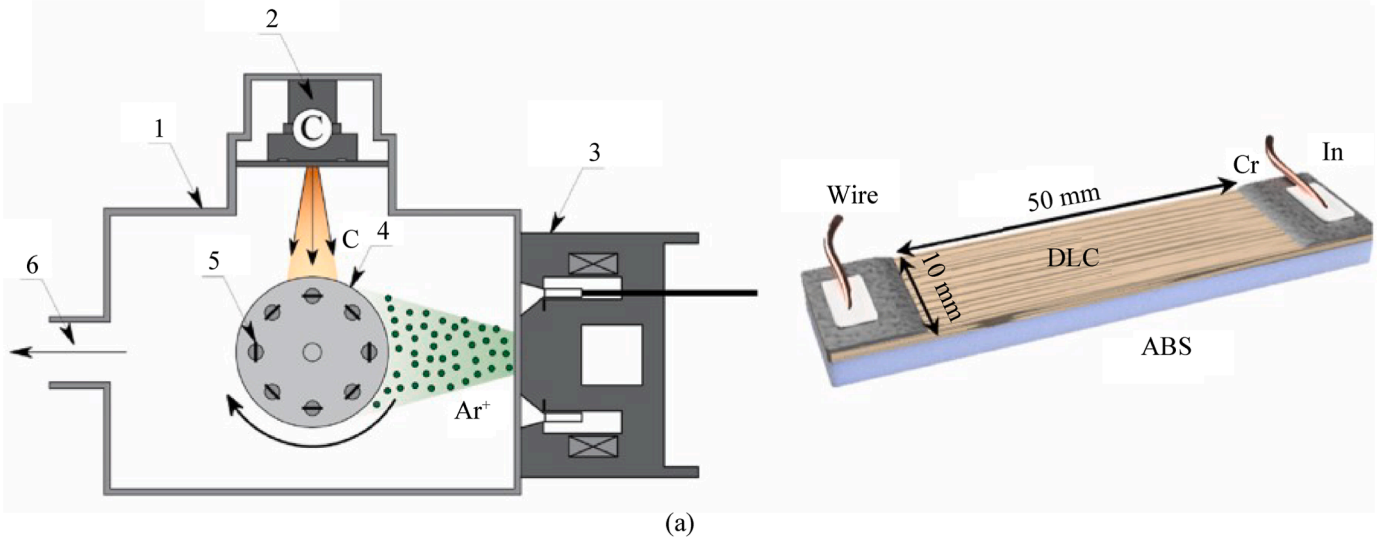

(a)

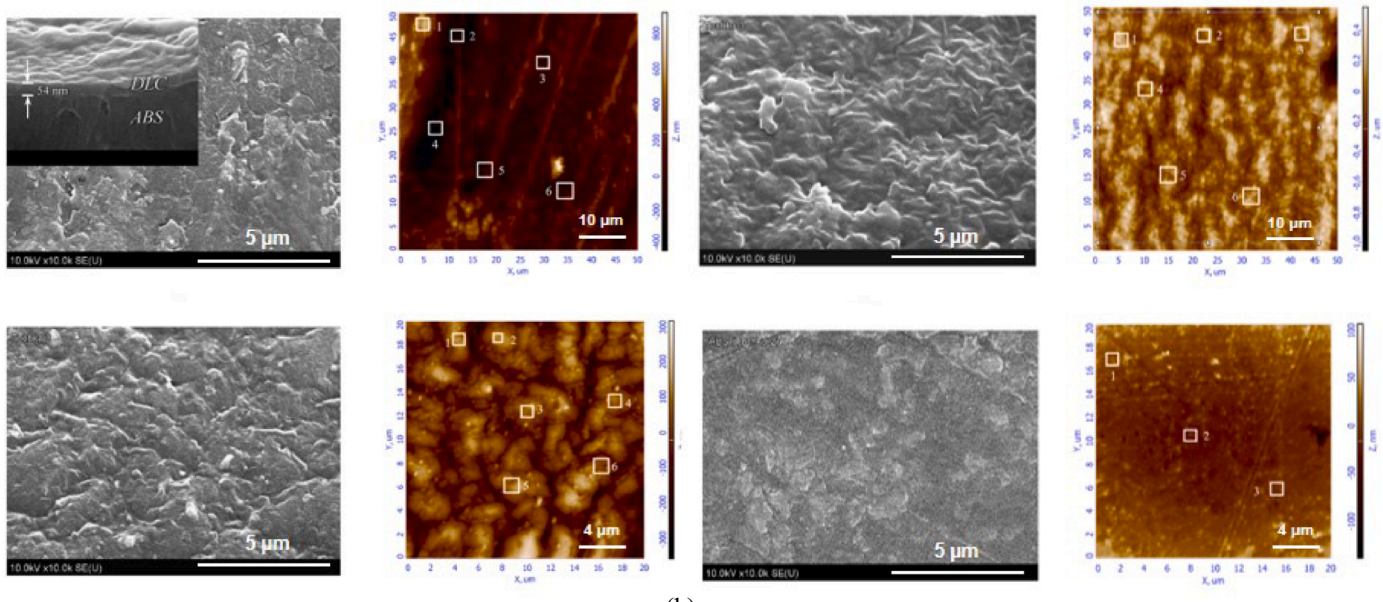

(b)

Fig. 7. (a) Schematic diagram of the DLC coating deposition device; (b) SEM and AFM images of the DLC coating surface and substrate surface [93].

pressure piston pumps and other equipment through multi-phase collaborative strengthening, self-lubricating phase design, and other optimizations [95,96].

High-entropy alloy coatings have emerged as transformative wear-resistant materials, leveraging their unique multi-principal element design strategy to overcome the performance limitations of conventional binary and ternary alloys [97,98]. The high-entropy stabilization mechanism facilitates the formation of a multiphase architecture combining solid-solution matrices with intermetallic phases, engineered through magnetron sputtering or laser cladding processes. This structural configuration synergistically enhances hardness and thermal stability, while the chemical complexity enables in-situ formation of adaptive oxide tribofilms under frictional stress [99,100]. Compared to traditional coatings, HEA coatings demonstrate superior wear resistance through a combination of dislocation entanglement, lattice distortion effects, and self-lubricating oxide layer formation, effectively mitigating adhesive and abrasive wear mechanisms in extreme environments [101]. These microstructure-property correlations position HEA coatings as critical surface engineering solutions for hydraulic systems requiring concurrent optimization of energy efficiency, component longevity, and operational safety [102,103].

Refractory high entropy alloys (RHEAs) have broad application prospects due to their excellent mechanical properties, but how to reduce friction and wear while maintaining high hardness is a major challenge. The NbMoWTa/Ag multilayer film significantly reduces the friction coefficient and maintains high hardness by introducing an Ag layer as a lubricating phase. Luo [103] presents a breakthrough through architecturally designed NbMoWTa/Ag multilayer films fabricated via precisely controlled magnetron sputtering, where periodic insertion of Ag lubricant layers achieves synergistic microstructure-property optimization. Cross-sectional SEM reveals a fundamental microstructural transition: films with $h > 5$ nm exhibit distinct laminar architecture with disrupted columnar growth, while coherent columnar structures spanning the entire thickness emerge at $h \leq 5$ nm through interfacial stress modulation (Fig. 8). The ultra-thin ($h = 2.5$ nm) multilayer configuration combines nanocrystalline NbMoWTa matrices (surface roughness $Ra = 3$ nm by AFM) with continuous Ag interlayers, generating coherent interface-induced dislocation blocking and Ag-mediated shear localization. This structural engineering enables hardness retention concurrent with ultra-low friction through in-situ formation of Ag-rich tribofilms, EDS mapping confirms elemental homogeneity without segregation (Fig. 8). The $h = 2.5$ nm multilayer demonstrates optimal tribo-mechanical balance, establishing a novel paradigm for self-lubricating RHEA coatings through nanolaminate design that couples structural coherence with phase-transition lubrication mechanisms.

3. Tribology performance of coatings for key friction parts

3.1. Metal coating

Bronze-based coatings have emerged as critical surface engineering solutions for axial piston pump tribo-components (e.g., cylinder/valve plate interfaces) operating under elastohydrodynamic lubrication (EHL) conditions, where interfacial failures cause catastrophic wear and energy losses [104]. Hao et al. [105] systematically compared PVD- and CVD-fabricated bronze coatings on 38CrMoAl substrates against bulk ductile iron counterparts through tribological analysis. The PVD coating's superior performance stems from its architecturally optimized nanocomposite structure. Microporous architecture enables lubricant retention, enhancing boundary lubrication (Fig. 9(a)). Al-Cu intermetallic reinforcements are dispersed in a Cu matrix with balanced hardness and fracture toughness. In contrast, the softer CVD coating suffers three-body abrasion through microcutting-induced plastic deformation, while bulk ductile iron exhibits adhesive-to-abrasive wear transition due to hardness mismatch with brass counterparts (Fig. 9(a)). Crucially, the PVD coating's tribofilm evolution mechanism involving in-situ oxide formation and subsurface work hardening highlights the effectiveness of PVD coatings in improving wear resistance and reducing friction loss in mechanical systems.

Guo et al. [106] addressed bronze coating oxidation limitations in thermal spray processes by employing cold spray deposition to fabricate Sn-bronze coatings (Cu-6 wt% Sn and Cu-8 wt% Sn), systematically investigating Sn content and annealing effects on structure and property relationships. Cold-sprayed coatings exhibited strain-hardened nanocrystalline structures with increased hardness (Cu-8 wt% Sn > Cu-6 wt% Sn) through dislocation accumulation and Sn solid-solution strengthening. Post-annealing induced grain recrystallization and twin formation at flattened grain interfaces, particularly prominent in Cu-8 wt% Sn (HT8), which disrupted grain boundary continuity (Fig. 9(b)). Higher Sn content enhanced wear resistance via solution strengthening. Annealing amplified coefficient of friction (COF) due to twin-induced surface embrittlement, the wear rate shows an opposite trend (Fig. 9(b)). This inverse hardness-wear resistance correlation highlights the critical balance between dislocation strengthening and twin-governed-sprayed Cu-8 wt% Sn coatings with controlled crystallographic defects as optimal candidates for piston pump tribo-surfaces requiring wear durability.

Yin et al. [107] engineered laser-clad aluminum bronze coatings through energy density modulation, establishing a critical process, structure, and property nexus. At optimal energy density (42.4 J/mm^2), controlled melt pool dynamics achieved balanced surface flatness and dense α-κ phase composites with refined grains. Higher energy densities (> 53 J/mm^2)induced vapor recoil-driven melt pool instability, while lower values (< 35 J/mm^2) caused incomplete powder melting. Sufficient reaction time at 42.4–70.7 J/mm^2 promoted α and κ equilibrium phases. Rapid cooling below 35 J/mm^2 triggered β′ martensite formation with coarse grains. The 42.4 J/mm^2 exhibited peak hardness 341.72 HV and minimum wear rate 4.37×10^{-2} mm^3/(N·m) through κ-phase dispersion strengthening and grain boundary hardening (Fig. 10(a)). The findings decouple laser energy, microstructural hierarchy, and performance relationships, providing a theoretical foundation and practical guidance for advancing materials science and tribological applications.

Miguel [108] systematically studied the influence mechanism of atmospheric plasma spraying (APS) and cold spraying (CGS) processes on the structure performance relationship of aluminum bronze alumina composite coatings. The results has shown that the APS process forms a sheet-like alumina phase through high-temperature melt deposition, and its large-area layered distribution significantly improves the wear resistance of the coating (APS-11% alumina coating reduces wear rate by 46%), while the solid-state deposition of the CGS process results in fine alumina particles (CGS-13% only reduces by 22%), which are easily peeled off synchronously with the substrate during wear (Fig. 10(b)). Microstructure analysis shows that the flattened alumina phase of APS coating can effectively hinder the abrasive cutting path, while the spherical ceramic phase of CGS coating has limited strengthening effect due to the lack of mechanical interlocking. Under corrosive conditions, the wear rate of APS composite coating increases with the increase of ceramic content due to preferential corrosion at the alumina and substrate interface, while CGS coating maintains stable wear performance due to its dense

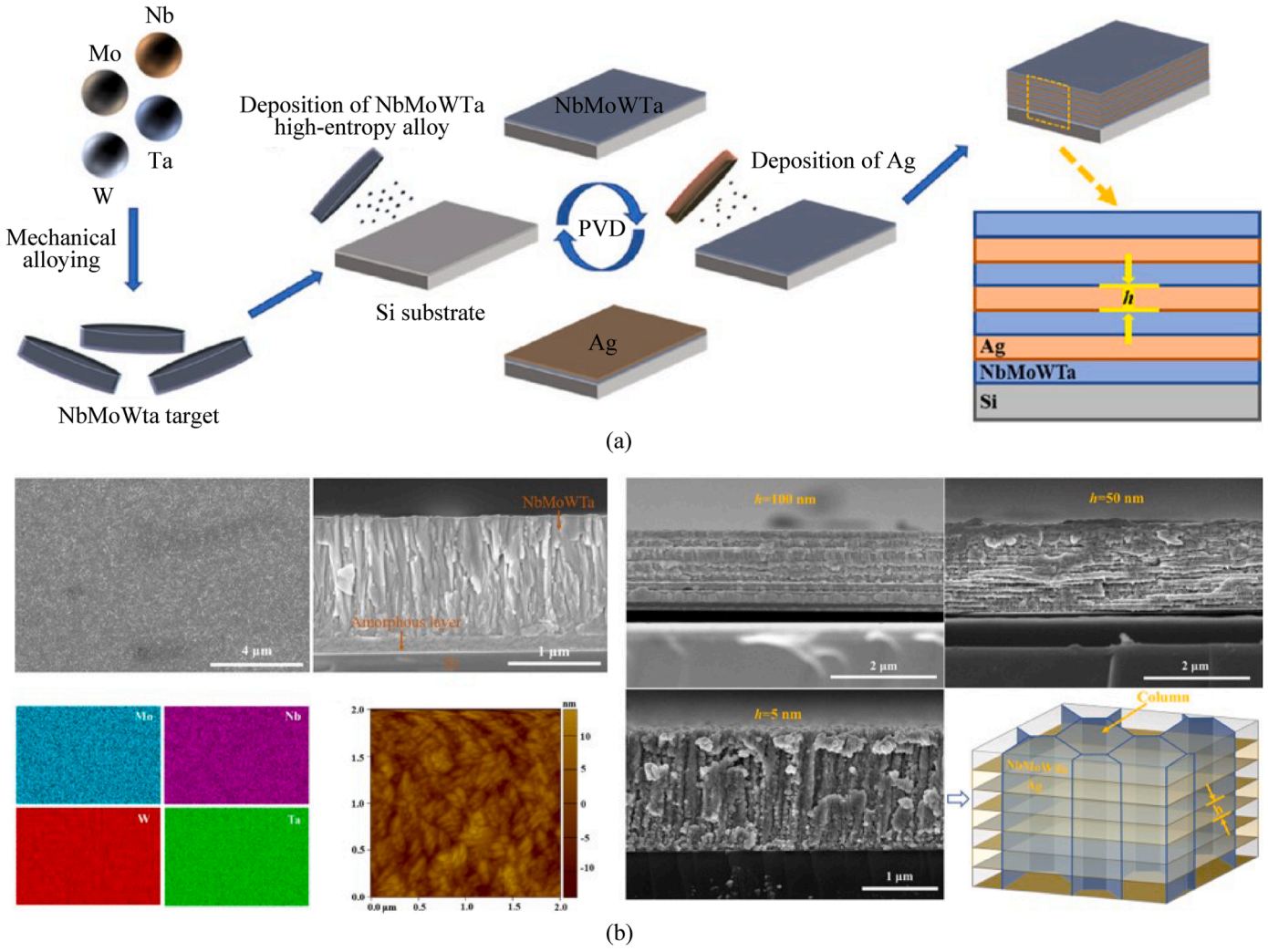

Fig. 8. (a) Schematic diagram illustrating the fabrication of the multilayer film with alternating layers of NbMoTaW RHEAs and Ag; (b) Microstructure of the NbMoTaW RHEA film and NbMoWTa/Ag multilayers [103].

structure. The thermodynamic spraying process dominates the wear mechanism and performance evolution of coatings by regulating the morphology and distribution of ceramic phases, providing a theoretical basis for the process structure synergistic optimization of wear-resistant coatings.

Das et al. [48] systematically investigated the structure and property correlation in HVOF-sprayed 10 wt% diamond-reinforced bronze coatings on bearing steel substrates. The study revealed that the HVOF process combined with ball-milled diamond-bronze powders enabled dense coating formation (< 1.5% porosity) with homogeneous diamond dispersion. Diamond incorporation induced significant dispersion strengthening, elevating microhardness and elastic modulus by 35% and 15%, respectively, through dislocation pinning effects. This structural modification shifted the dominant wear mechanism from plastic deformation in pure bronze coatings to controlled brittle delamination in composites, reducing the coefficient of friction by 65%. Notably, the composite's enhanced hardness induced larger counterpart wear scars while its limited ductility suppressed metallic transfer layer formation, contrasting with the continuous plastic flow-mediated transfer in pure bronze. The research demonstrates that HVOF processed diamond-bronze coatings achieve progressive wear resistance enhancement through synergistic "hard-phase constrained dislocation motion – matrix stress distribution", providing critical insights for designing high-load tribological coatings via particle-reinforced architecture optimization.

In further research, Miguel et al. [109] prepared aluminum bronze composite coatings with different alumina contents using plasma spraying technology. Adding alumina to the bronze coating significantly improved its wear resistance. Researchers have proposed an additional wear mechanism unique to composite coatings to explain this enhancement. The fracture of alumina flakes directly beneath the worn track resulted in uniform alumina particles embedding in the bronze matrix. This process improves surface hardness and effectively suppresses wear. In addition, debris composed of copper and aluminum oxide accumulates on the wear track, further reducing coating wear. By enhancing the structure and disrupting the wear process through debris deposition, composite coatings exhibit better wear resistance, providing valuable insights for the development of advanced frictional materials.

3.2. Ceramic coating

Nitride-based cermets are predominantly utilized in applications involving piston pumps, with nitriding serving as the

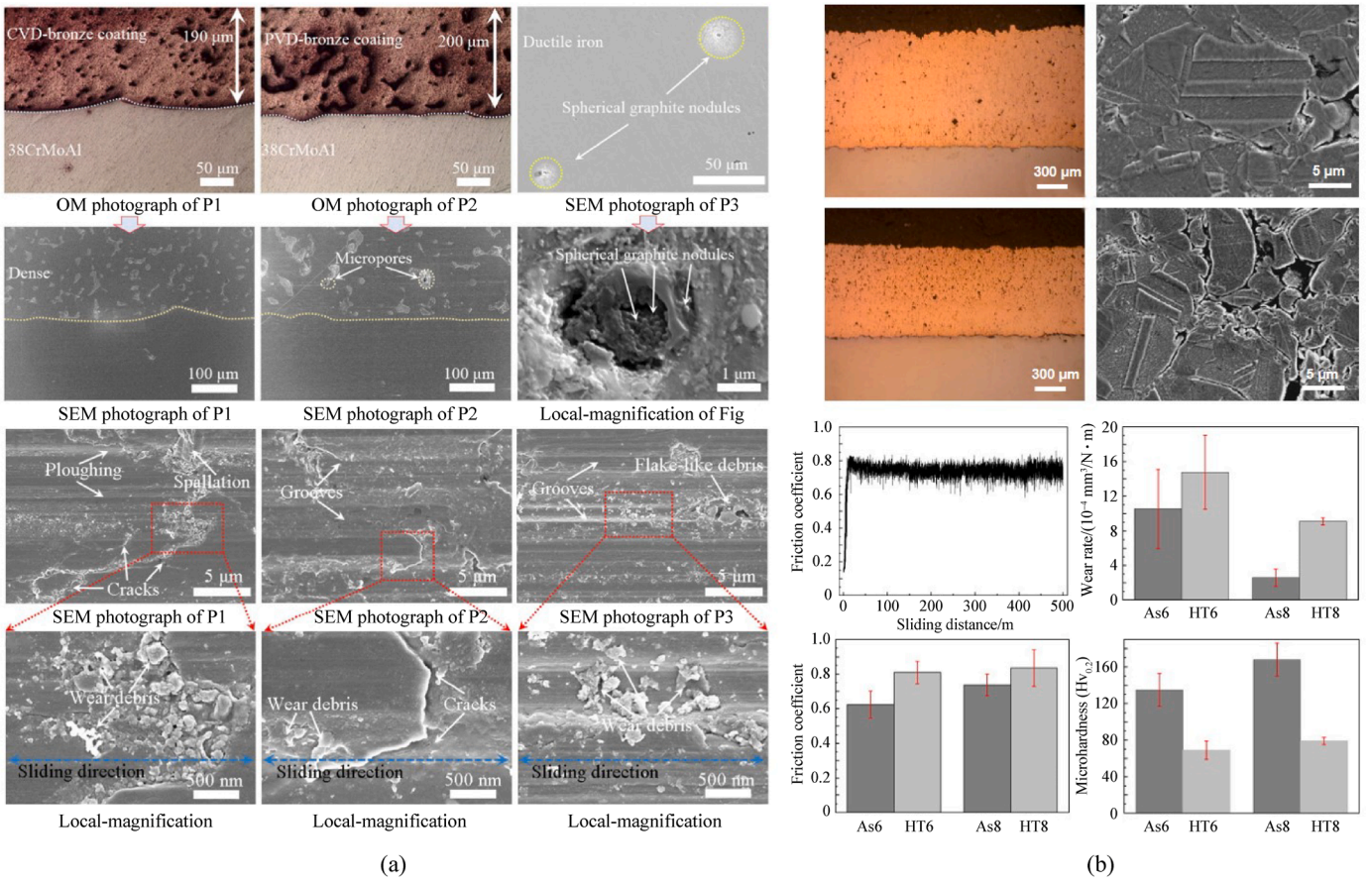

Fig. 9. (a) Cross-sectional microstructural characterization of CVD deposited bronze coating (P1), PVD deposited bronze coating (P2), and ductile iron substrate (P3) [105]; (b) Cross-sectional microstructure of the heat-treated bronze coatings and tribological properties of bronze coatings under different treatments [106].

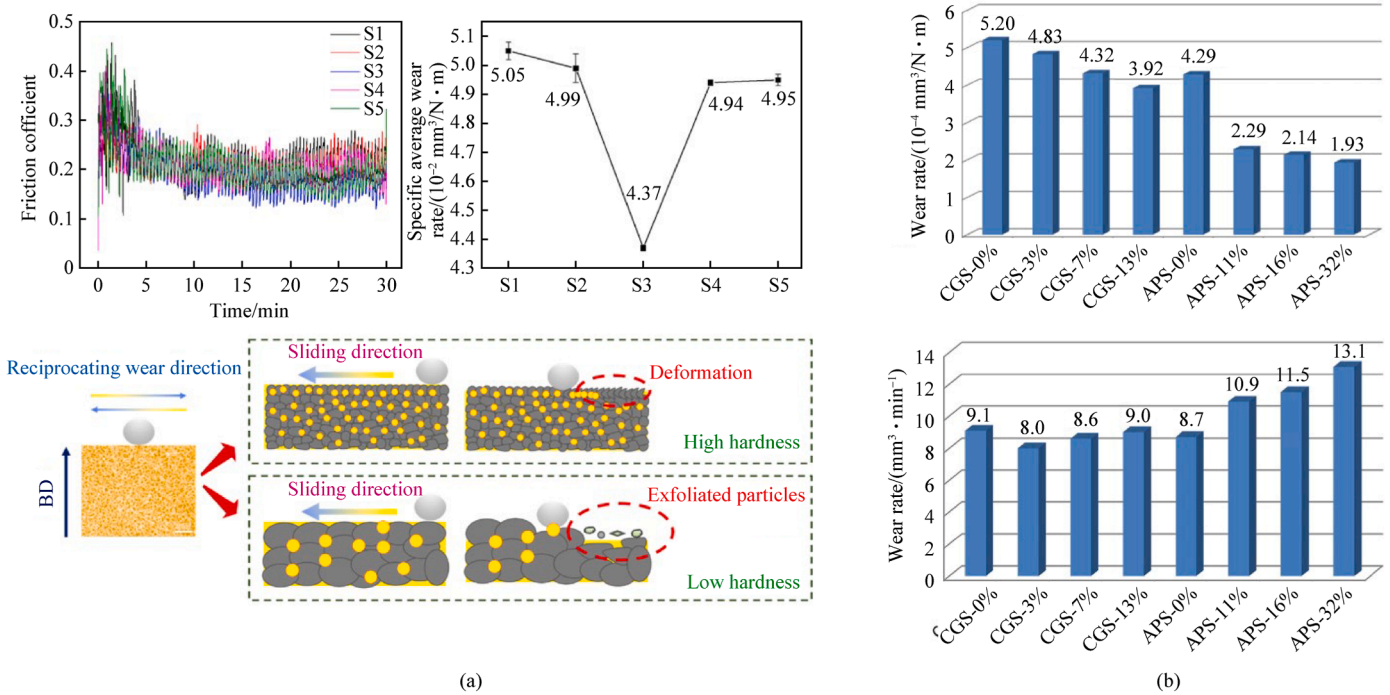

Fig. 10. (a) Tribological performance of aluminum bronze coatings under varying laser energy densities and Schematic diagram of the reciprocal wear mechanism of aluminum bronze coatings fabricated by laser fusion cladding [107]; (b) Rubber wheels to test the wear rate of different coatings and corrosion wear rate [108].

cornerstone technology [110]. Nitriding is a surface modification process wherein nitrogen atoms diffuse into the metal surface, forming a nitride-reinforced layer. This process significantly elevates the material's surface hardness, wear resistance, and corrosion resistance [111]. Furthermore, nitrocarburizing, also known as soft nitriding, represents an advanced surface strengthening technique. This process involves introducing carbon-containing gases, such as carbon dioxide or acetylene, during the nitriding cycle to achieve the simultaneous diffusion of nitrogen and carbon atoms at comparable temperatures. Compared to traditional carburizing, nitrocarburizing operates at lower temperatures and causes minimal workpiece deformation [112,113]. Additionally, the incorporation of active carbon atoms further optimizes the material's comprehensive properties, offering a superior balance of hardness and ductility [114,115]. In practical applications, these cermets are often applied as coatings at critical interfaces within mechanical systems. For example, coatings such as TiN, TiCN, CrSiN, CrZnN, and ZrCg are deposited at the juncture between the cylinder block and valve plate. These coatings, characterized by their ceramic reinforcement and metal bonding, possess both high hardness and high toughness. This unique combination significantly enhances wear resistance, thereby prolonging the operational life of mechanical components and improving overall system efficiency [116].

3.2.1. Binary nitride cermet coatings

Binary nitride cermet coatings cleverly merge the benefits of metallic and ceramic materials, typically composed of two primary components, such as AlN and SiN [117,118]. These components effectively blend the toughness inherent in metals with the remarkable strength and hardness of ceramics. The importance of binary nitride cermet coatings in tribology is chiefly illustrated by their superior wear resistance, high-temperature stability, and corrosion resistance [119]. These attributes have facilitated their widespread use across various industries, including aerospace, automotive manufacturing, energy equipment, and industrial machinery. As coating technology continues to evolve and improve, binary nitride cermet coatings are poised to assume an increasingly vital role in tribology research and applications, strongly propelling mechanical systems toward enhanced efficiency, extended service life, and environmental sustainability.

Hong [120] deposited TiN coatings on the surface of the cylinder barrel of an axial piston pump, and the test showed that: 300 bar load, 100 rpm, the TiN coating reduced the friction torque of the valve plate by 78% (efficiency improvement of 1.3%), and the wear rate decreased by 45%–50%; This study emphasizes that TiN coating significantly reduces the friction and wear between cylinder barrel and valve plate, and improves the efficiency and durability of hydraulic pumps, especially under low-speed and high-pressure operating conditions. The application of PVD coating technology on cylinder barrel surfaces is practical and promising.

Lee [121] engineered duplex TiN coatings on AISI 4340 steel through reactive magnetron sputtering, integrating plasma nitriding with PVD to establish a hierarchical surface architecture for EHA pump components. The duplex system synergized a plasma-nitrided diffusion zone with a columnar-structured TiN top layer, achieving exceptional tribological performance under extreme conditions. As illustrated in Fig. 11, the duplex coating achieved an ultralow static COF of 0.04 compared to plasma-nitrided counterparts. Structural analysis revealed that while both monolayer and duplex TiN coatings exhibited abrasive wear patterns, the bilayer architecture maintained surface integrity through its composite design. The nitrided interlayer provided mechanical support, while the graded TiN coating minimized asperity contact. This synergistic structure resulted in a wear rate 1.8 × lower than monolayer TiN and an order of magnitude reduction versus plasma-nitrided specimens. Scratch tests confirmed enhanced adhesion in the duplex system due to interfacial stress mitigation. Notably, the coating's ultra-low static COF addressed critical limitations in pump start-up and low-speed operation by preventing adhesive wear between steel/bronze tribopairs. This work demonstrates that functionally graded surface engineering combining diffusion hardening and PVD coatings enables simultaneous optimization of load-bearing capacity, interfacial adhesion, and tribological properties, crucial for developing energy-efficient hydraulic systems with extended service life.

3.2.2. Multiple nitride cermet coatings

As an advanced surface functional material system, ternary TiCN ceramic coatings have established an important position in the engineering field after three decades of development [122]. These coatings are notable for their ultra-high microhardness, ranging from 30 to 40 GPa, excellent wear and corrosion resistance, and stable physicochemical characteristics, making them suitable for industries where mechanical stress and harsh conditions are common [123,124]. Compared to traditional TiCN materials, PVD-based coatings provide significant advantages, enabling uniform coverage and overcoming size limitations [125]. Further research into their manufacturing processes, cost scalability, and real-world applications would provide deeper insights into their practicality and widespread adoption across various industries [126].

In the operation of axial piston pumps, the sliding contact between the steel-based cylinder barrel and the soft bronze valve plate is prone to rapid wear due to unstable lubrication. To address this tribological challenge. Lee et al. [127] demonstrated that CrSiN coatings deposited on cylinder barrel surfaces significantly enhance tribological performance in hydraulic piston pumps under low-speed mixed lubrication and high-pressure conditions. Comparative friction analysis revealed that Condition II (CrSiN-coated surfaces) exhibited > 50% reduction in COF versus Condition I (conventional nitrided surfaces). This performance enhancement originates from the coating's engineered microstructure, where Si segregation promotes the in situ formation of a $Si(OH)_2$ self-lubricating tribofilm during operation. The nanocomposite coating architecture achieves load-independent friction behavior (Condition II), contrasting with the load-sensitive COF of uncoated surfaces (Condition I). Surface characterization confirms the synergistic effect of reduced roughness and boundary lubrication mechanisms from the tribofilm. These microstructure-property correlations validate CrSiN coatings as a surface engineering solution for improving hydrodynamic efficiency in axial piston pumps through tailored solid lubricant architectures. It should be noted that CrSiN coatings maintain low friction characteristics in dry environments, but high humidity environments are prone to lubrication film failure due to water molecule adsorption, leading to an increase in friction coefficient. At the same time, the coating and substrate need to match thermal expansion and mechanical properties to reduce interfacial stress, and the introduction of gradient transition layers can improve compatibility and reliability.

Lee et al. [128] systematically investigated silicon doping effects on Cr-Si-N coatings deposited via unbalanced magnetron sputtering on AISI 4340 steel, focusing on structure and property relationships. With increasing silicon content to 9.8 at%, the coatings achieved a peak hardness of 24.2 GPa through grain refinement governed by the Hall-Petch effect and structural densification. The optimized coating demonstrated exceptional

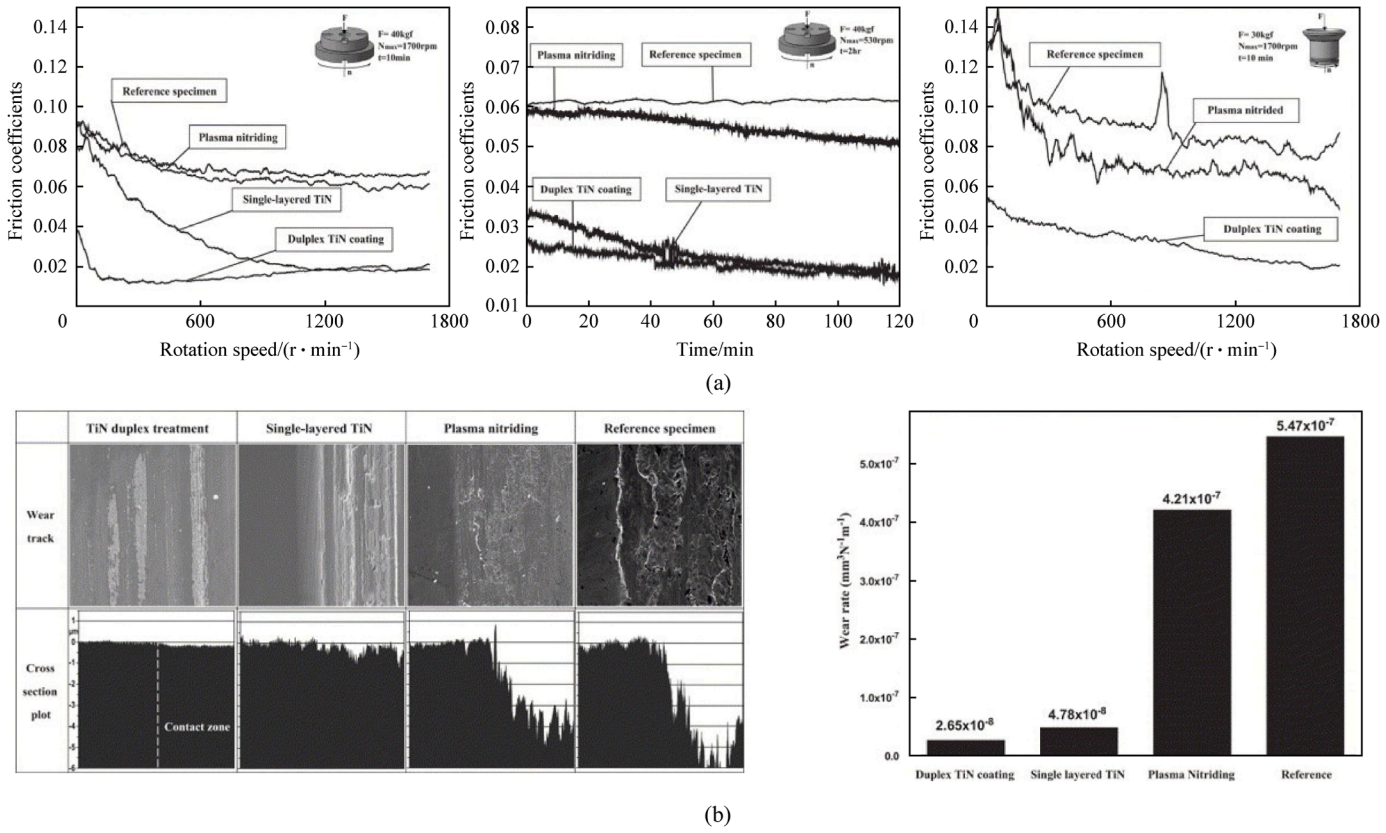

Fig. 11. (a) The Stribeck curves of the test specimen and the friction coefficient curves; (b) The wear tracks and wear rate of various specimens after wear test [121].

tribological performance with a static COF of 0.044 under low-speed or high-load conditions, outperforming CrN (0.09), TiN (0.11), and plasma-nitrided counterparts (0.18). This enhanced wear resistance stems from a silicon-induced nanocrystalline structure that suppresses grain boundary sliding. Dense microstructure minimizing defect propagation and in situ formation of lubricious silicon oxide tribolayers during wear. The study establishes that controlled silicon incorporation through magnetron sputtering enables simultaneous optimization of mechanical and tribological properties in transition metal nitride coatings.

In addition, Kim et al. [129] engineered ternary $Cr_{1-x}Zr_xN$ coatings ($0 \leq x \leq 0.34$) via closed-field unbalanced magnetron sputtering, correlating Zr-content-dependent structural evolution with enhanced mechanical performance. Structural analysis revealed (Fig. 12) a maximum hardness of 34 GPa and elastic modulus of 425 GPa at $x = 0.25$, attributed to solid-solution strengthening from Zr substitution in the CrN lattice, which induced compressive lattice strain and suppressed dislocation motion. The hardness degradation beyond $x = 0.25$ stemmed from Zr oversaturation, triggering phase segregation and diminished crystallinity. Tribological assessments demonstrated superior wear resistance for $x = 0.25$ coatings, exhibiting smooth wear tracks and no delamination.

Hong and Lee [130] investigate that CrZrN coatings demonstrated superior tribological performance under severe operating conditions compared to CrSiN counterparts, exhibiting a 0.35% increase in pump torque efficiency alongside reduced COF and enhanced wear resistance. This performance enhancement stems from a CrZrN-optimized densified grain structure and improved mechanical properties, which enable better load pressure adaptability through enhanced cohesive strength between columnar crystallites. Notably, the coating's failure mechanism shows strong microstructure dependence, where reduced porosity effectively inhibits corrosive media permeation through interconnected pore networks. Rosso et al. [131] revealed that Ti-induced phase stabilization maintained HV at 18–22 GPa in corrosive media, while plasma-assisted seal post-treatment created a dense diffusion barrier. This surface engineering strategy enhanced wear and corrosion resistance and fracture toughness through porosity reduction, residual stress modulation, and solid lubricant phase formation.

Aktarer et al. [132] systematically investigated TiSiN and AlTiCrN coatings deposited via cathodic arc evaporation on gray cast iron cylinder liners, correlating microstructure-property relationships with tribological performance under varying loads and environments. Under dry sliding conditions (Fig. 13), both coatings exhibited distinct load-dependent friction mechanisms. TiSiN nanocrystalline composite structure delivered superior low-load performance through enhanced hardness and anti-plastic deformation capability, while AlTiCrN with coherent CrN and TiN interfaces demonstrated high-load durability via improved adhesion strength and crack propagation resistance. AlTiCrN dominance across all loads is attributed to its lower surface energy, promoting boundary lubrication stability and tribo-oxidative film formation. TiSiN for normal operation to leverage its surface integrity preservation, and AlTiCrN under severe lubrication conditions to exploit its adaptive oxide layer formation and interfacial stress dissipation capabilities, collectively addressing gray cast iron's inherent tribological limitations in combustion engines.

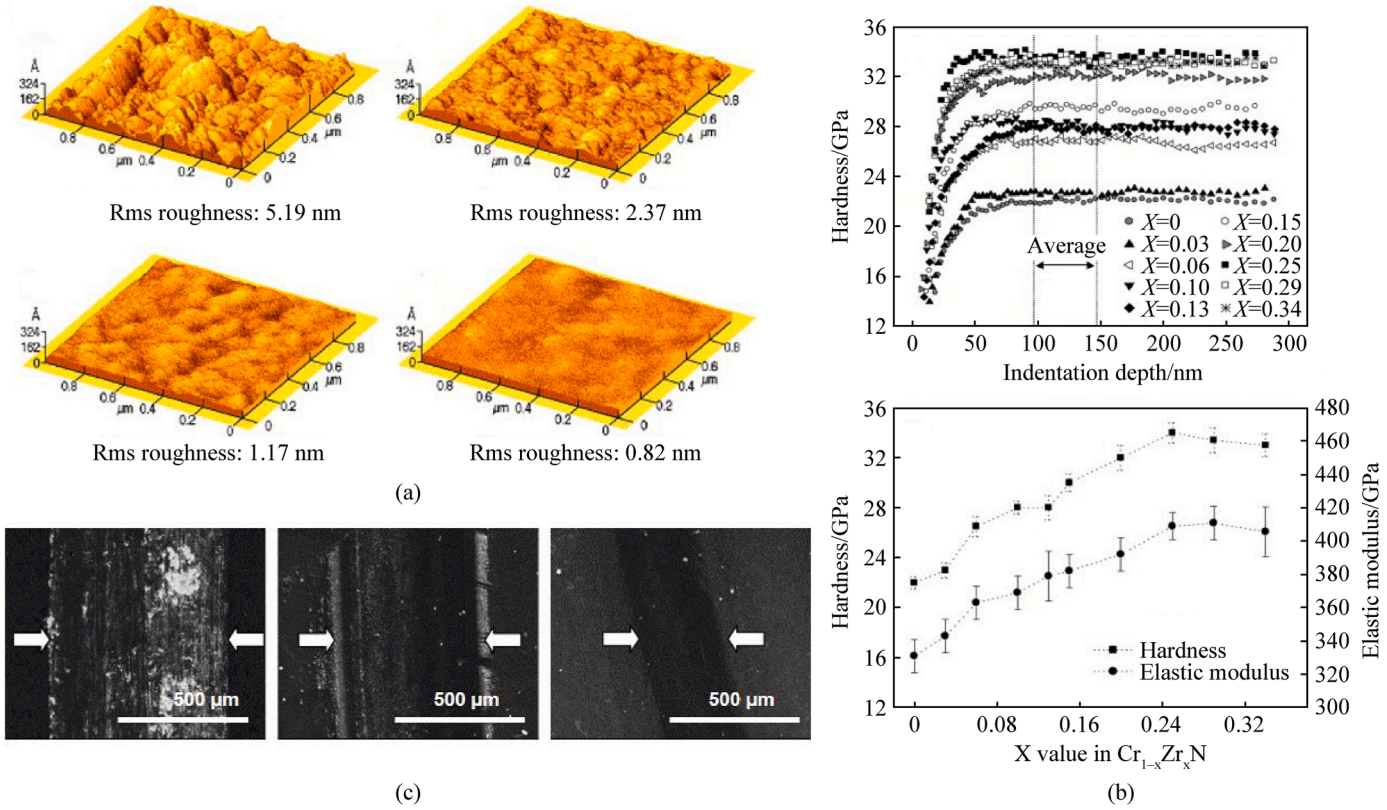

Fig. 12. (a) AFM surface morphologies and Rms roughness of the $Cr_{1-x}Zr_xN$ films; (b) Hardness and elastic modulus of the $Cr_{1-x}Zr_xN$ films as a function of the Zr content (x value); (c) SEM micrographs of wear tracks: From left to right, they are substrate (nitrided AISI H13 steel), CrN ($x = 0$) film and $Cr_{1-x}Zr_xN$ ($x = 0.25$) [129].

3.3. Diamond-like carbon

Electrostatic actuator pumps, serving as regulatory elements to compensate for position control errors, face critical tribological challenges from intermittent operation modes. These pumps require enhanced resistance to extreme friction compared to conventional pumps, which operate continuously at high speeds. It has been demonstrated that mixed friction significantly increases frictional power loss and accelerates wear rates of sliding components, such as pistons [133]. To address this problem, Hong et al. [134] demonstrated that swash plates coated with DLC can effectively reduce both the COF and wear rate of the piston shoe's contacting surface. Furthermore, it enhances leakage flow control by applying the coating to the piston swash plate and ball joint surfaces. When both DLC-coated swash plates and ball joints are employed, the total power loss of hydrostatic piston shoe bearings is reduced by over 40% at pump speeds below 100 rpm. In addition, Kalin [135] showed that DLC-coated piston shoes exhibit significantly lower surface roughness after run-in, with systematic debris generation reduced by more than 50% compared to conventional steel systems. Additionally, the degree of lubricant oxidation is notably reduced, which effectively extends the oil's service life.

Schuhler [136] conducted research on surface treatment on swashplate steel, demonstrating that nitrided materials exhibit superior wear resistance under both dry friction and lubrication conditions, with performance being particularly notable in lubrication scenarios. Manhabosco [137] developed graphite-like a-C:H thin films on the surfaces of both nitrided and non-nitrided Ti6Al4V alloys using radio-frequency plasma-assisted chemical vapor deposition. Contrasting performance between nitrided and bare alloys to elucidate structure and tribocorrosion relationships. The a-C:H films demonstrated superior tribological performance. However, during the wear-corrosion tests, the films sustained significant damage and formed transfer layers. The surface morphology of the wear traces revealed distinct delamination, surface deformation, and ploughing at the film boundaries (Fig. 14(a)). The test results indicated that the service life of the films on nitrided substrates was reduced by a factor of four compared to untreated substrates under the combined influence of load and corrosion media. This degradation primarily stemmed from the relatively weak interfacial bonding strength between the GLCH film and the nitrided substrate, which facilitated the penetration of corrosive media along the interface, ultimately triggering film spalling. Furthermore, it highlights the critical importance of understanding the failure mechanisms when load and corrosion environments act simultaneously.

Dalibón [138,139] investigated plasma-assisted CVD-deposited DLC coatings (~37 μm) on nitrided and untreated AISI 316L substrates, elucidating critical structure and property relationships. While abrasive wear tests showed comparable mass loss reductions for both systems due to DLC inherent lubricity (Fig. 14(b)). Conversely, in the erosive wear test, the nitrided specimens exhibited lower mass loss than the others, attributed to the expanded austenite layer, which enhances load-carrying capacity and wear resistance. Electrochemical analysis revealed the duplex system's superior corrosion resistance. Nitriding-induced surface roughening improved mechanical interlocking, increasing adhesion strength. For duplex systems under combined tribocorrosion stresses, confirming that the nitrided interface's optimized hardness gradient and defect-blocking capability outweigh the DLC intrinsic porosity limitations. These findings establish substrate

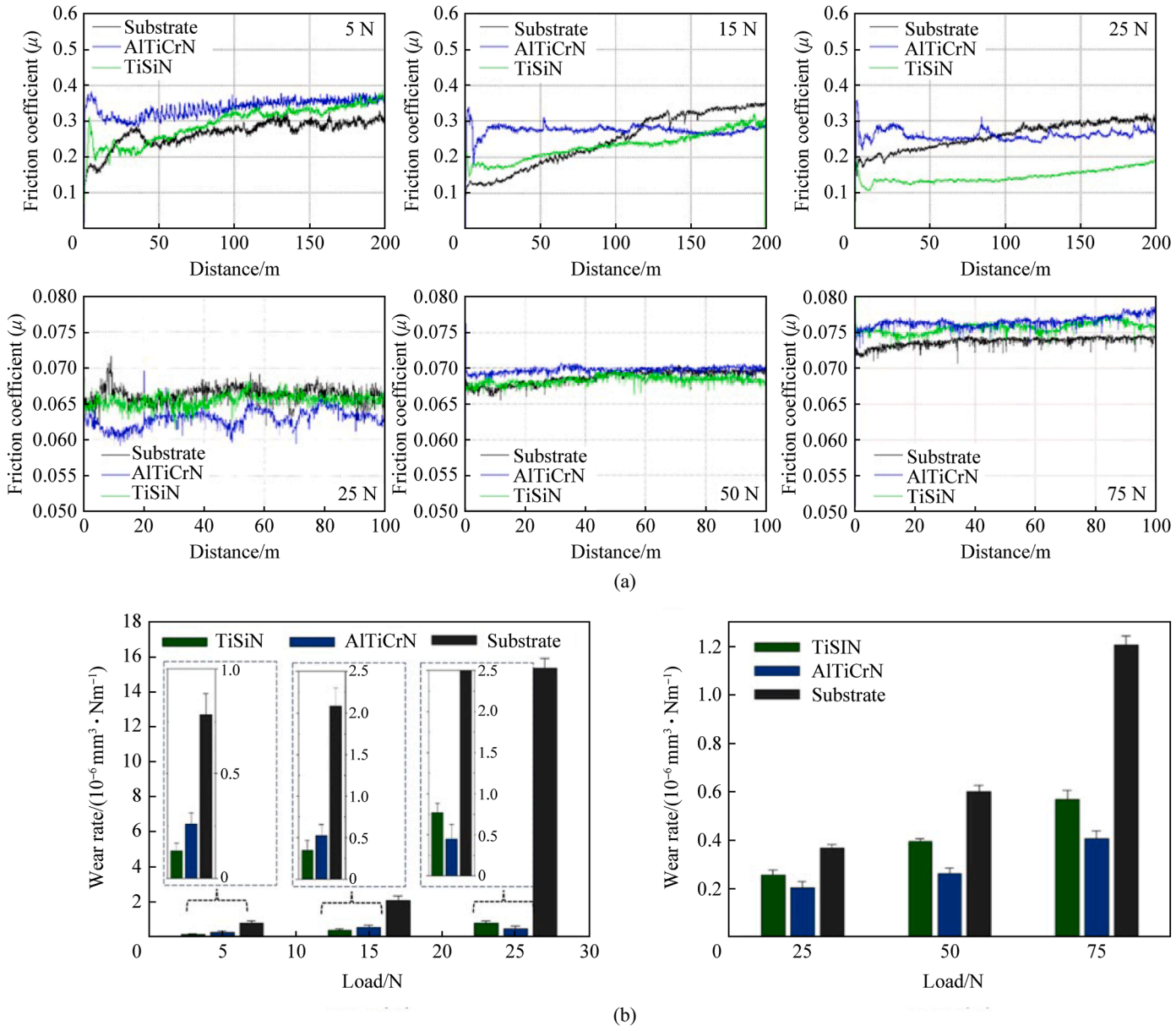

Fig. 13. (a) The substrate, TiSiN, and AlTiCrN coatings COF curves under dry conditions and lubricated sliding conditions; (b) Wear rates of coatings and substrate under dry and lubricated conditions [132].

preconditioning through nitriding as a critical strategy for engineering erosion-corrosion resistant DLC coatings via synergistic control of stress distribution and electrochemical compatibility.

As a new type of superelastic material, 60NiTi alloy meets the performance requirements of aerospace bearing materials, but its tribological performance is poor, especially under dry sliding conditions [141]. Zhou et al.'s [140] study demonstrates that ion-beam-enhanced magnetron-sputtered H-DLC coatings fundamentally improve the tribological performance of superelastic 60NiTi aerospace alloys through optimized structure. Nanoindentation revealed the H-DLC exceptional mechanical behavior with high H/E and H^3/E^2 ratios, indicating superior elastic strain tolerance and plastic deformation resistance (Fig. 14(c)). The coating maintained stable hardness up to 40 mN load despite modulus reduction, demonstrating effective load accommodation through the superelastic substrate's reversible phase transformation. This performance enhancement stems from Strong interfacial adhesion enabled by ion-beam-induced substrate activation, preventing coating delamination. These findings establish H-DLC and 60NiTi as a paradigm for extreme-condition tribological systems, where engineered coating and substrate interactions combine surface hardness with bulk elasticity through controlled interface physics and stress-state matching.

3.4. High-entropy alloy (HEA) coatings

Since the research team led by Yeh introduced the concept of multi-major element alloying, the Gibbs free energy reduction effect triggered by high configurational entropy has effectively facilitated the formation of a single solid solution structure, such as the face-centered cubic phase. Over the past decade, HEA systems like CoCrNi and CoCrFeNiMn have gained prominence in

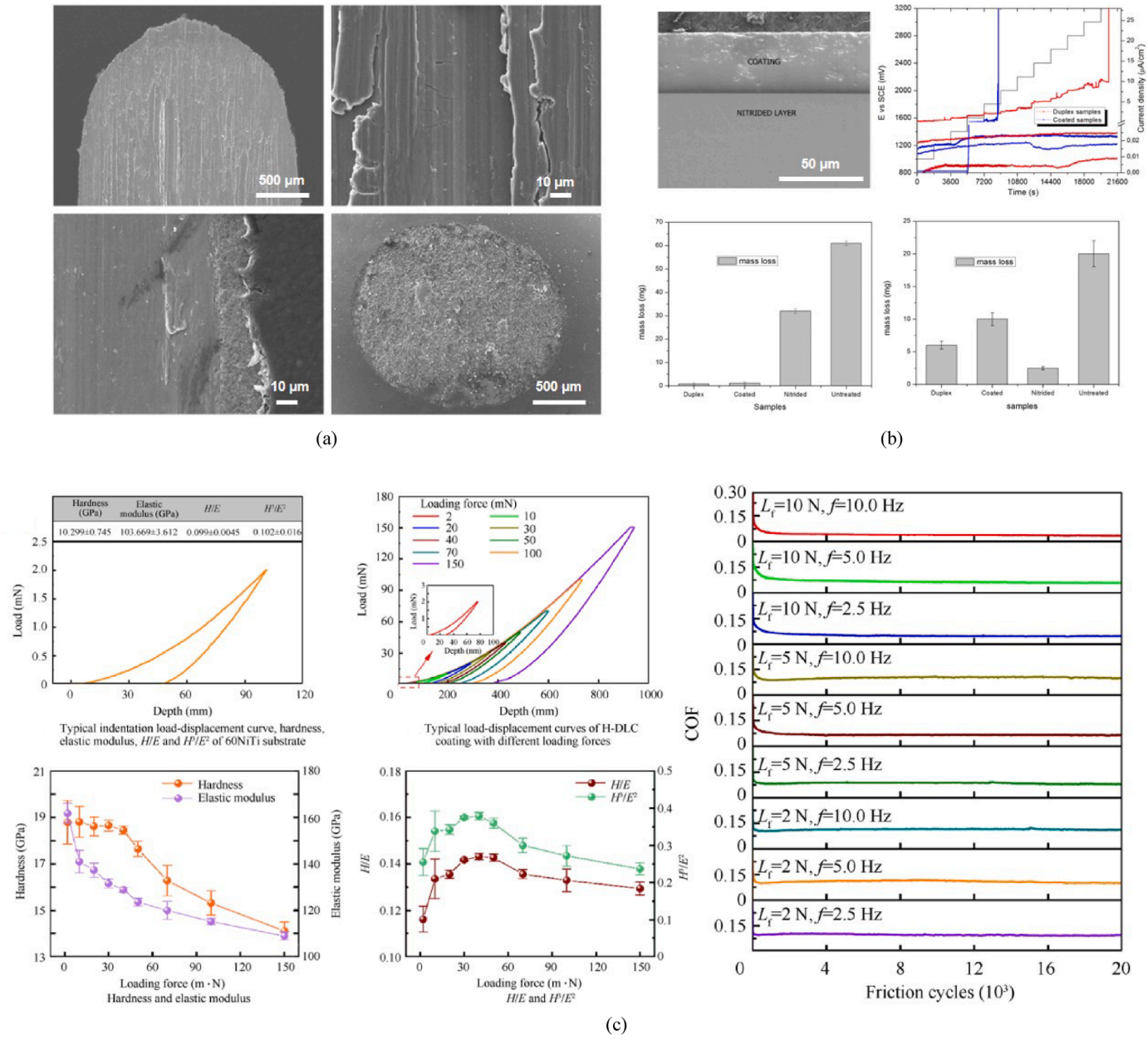

Fig. 14. (a) SEM images of the wear track after 2 h of wear–corrosion test at OCP for nitrided alloy covered by DLC [137]; (b) Morphology of biphasic DLC coatings, mass loss of samples treated under different conditions and potential and current density of duplex and coated samples [139]; (c) Mechanical behaviors of 60NiTi and H-DLC coating and COF of H-DLC coating with different friction loads and frequencies [140].

materials science research, owing to their exceptional strength, hardness, and wear resistance [142,143]. Wang et al. [144] developed hierarchical CoCrNi-Al_2O_3-Ni/MoS_2 composites, achieving ultralow-temperature adaptability through grain refinement and deformation twinning reinforcement mechanisms. Compared to traditional CoCrNi-Al_2O_3 composites, its wear resistance increased by 14.8 times, with a stable wear rate of 6.78 $\times$ 10^{-5} $mm^3/(N{\cdot}m)$ (Fig. 15), demonstrating exceptional adaptability to extreme operating environments.

Although cobalt-chromium-nickel iron-based HEAs demonstrate superior strain-hardening characteristics and tensile ductility, their limited wear resistance restricts their broader engineering applications. This drawback can be mitigated by incorporating graphene, a two-dimensional material with high strength, stiffness, low density, and self-lubricating properties [145,146]. Experimental results show that graphene reinforcement effectively reduces long-term wear in HEA-based friction systems [147,148]. Li et al. [149], demonstrated through molecular dynamics that the embedded graphene nano-sheets significantly inhibited sub-surface damage progression, and the strengthening mechanism transitioned from dislocation-graphene interaction-dominated to graphene morphology-dominated as the depth of the nano-sheets increased. In their investigation of interfacial behavior, Hua et al. [150] conducted a systematic atomic-scale simulation of the interfacial characteristics and dislocation evolution in the CoCrNi/Gr composite system. Hua identified six equilibrium interfacial stacking configurations, among which the three-part dislocation hybrid configuration at the triple junction exhibited the lowest stress state. The graphene, a moderate increase in the torsion angle enhanced strength, but exceeding a

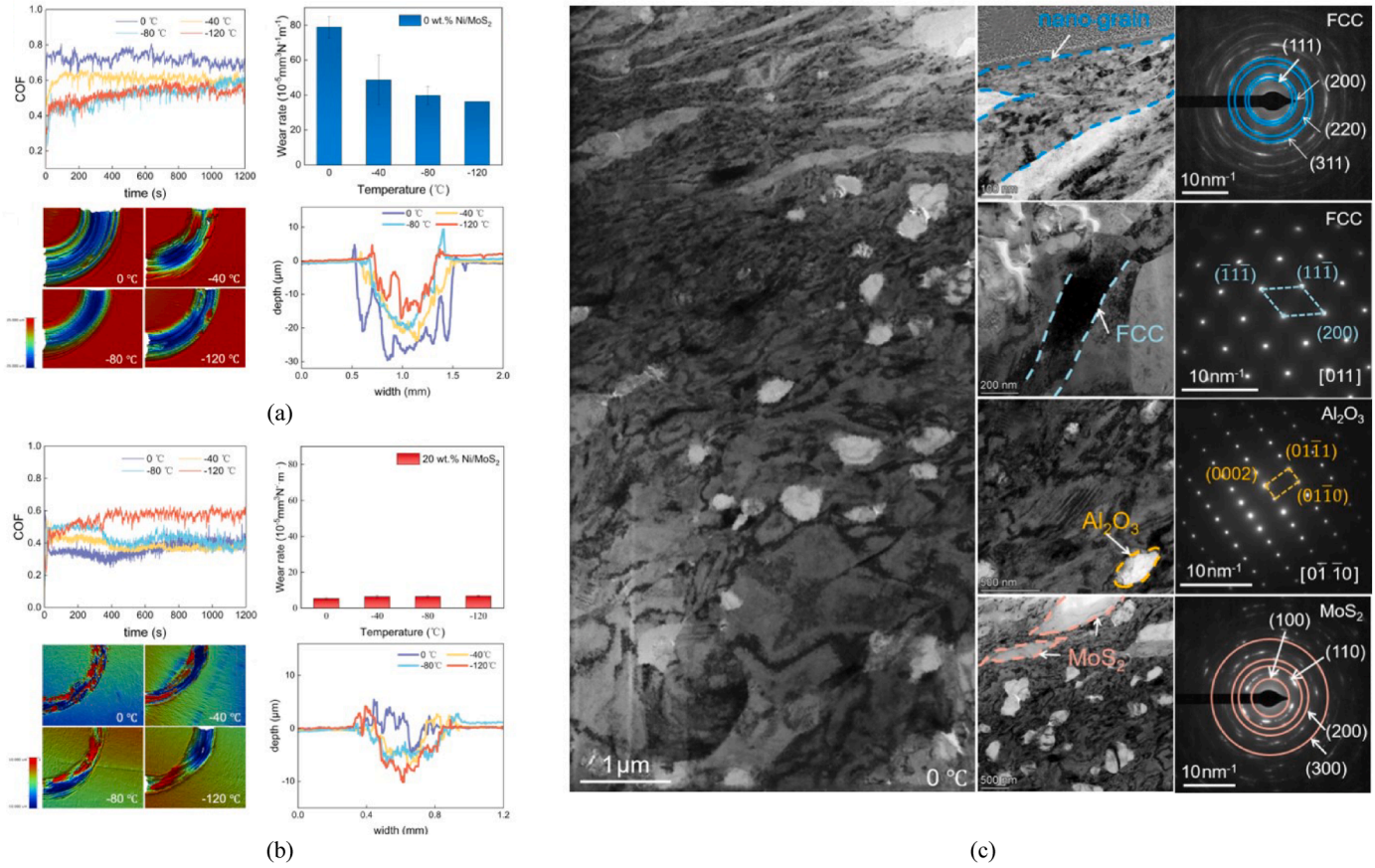

Fig. 15. (a) Tribological behaviors of 0 wt% Ni/MoS_2 composite under varying cryogenic temperatures; (b) TEM subsurface characteristics of the 20 wt% Ni/MoS_2 composite after wear test at 0 °C; (c) Tribological behaviors of 20 wt% Ni/MoS_2 composite under varying cryogenic temperatures [144].

critical value led to a significant drop in the composite system's yield strength due to the disappearance of interfacial dislocations. These findings provide critical scientific insights for the precise control of the HEA and graphene interfacial structure.

RHEAs, comprising refractory elements such as Nb, Mo, Ta, W, and V, exhibit exceptional strength and hardness under high-temperature and heavy-duty conditions due to the synergistic effects of their composition. These innovative materials demonstrate promising application potential in diverse industries, including aerospace, electronics, and automotive sectors. Notably, systems such as CrMoNbV and NbMoWTa alloys maintain superior mechanical properties even at extremely high temperatures, reaching up to 1,600 °C.

Jiao et al. [151] have successfully developed ultra-hard NbMoWTa thin films using the spinodal decomposition single-target sputtering technique. This technique enables the formation of a unique periodic alternating multilayer architecture through elemental segregation during deposition. Molecular dynamics and Monte Carlo simulations revealed that Ta–Mo and W–Nb atomic pairs exhibit strong chemical interactions. These interactions, combined with the periodic alternating stress fields within the film, synergistically inhibit dislocation motion, thereby enhancing mechanical performance. As a result, the films exhibit an ultra-high hardness of 21.9 GPa and a low wear rate of 1.2×10^{-5} $mm^3/(N{\cdot}m)$ (Fig. 16(a)). However, the intrinsic brittleness of refractory high-entropy alloys tends to cause surface cracking during frictional contact, leading to a discrepancy between the theoretical wear resistance and the actual performance. To overcome this limitation, researchers have proposed in-situ lubrication strategies to enhance surface stability and reduce the COF. Zhou et al. [152] validated this approach by employing $(NbMoWTa)_{1-x}Ag_x$ thin films fabricated via magnetron co-sputtering. Specifically, the $(NbMoWTa)_{75}Ag_{25}$ films exhibited a significant 54.3% reduction in the COF and an 81.6% decrease in the wear rate, attributed to the in-situ formation of a silver-based lubrication layer (Fig. 16(b)). This discovery offers a novel composite modification pathway for advancing high-performance RHEA films. Their findings demonstrate that carefully controlling the silver content enhances the tribological properties of materials while preserving the matrix's hardness.

4. Conclusions and prospects

Under light load dry conditions, coatings rely on surface lubricating films; heavy load scenarios necessitate reinforced phases to suppress plastic deformation. Corrosive or high temperature environments depend on dense oxide barriers, while extreme thermal conditions require matching the thermal expansion behavior between coating and substrate. This article systematically reviews the microstructure and performance correlation of metal, ceramic, DLC, and HEA coatings used in high-pressure piston pumps. Metal coatings adapt to medium low temperature and low pressure environments through mechanical interlocking and phase transformation strengthening, but have high temperature softening defects. In the future, it is necessary to develop high temperature resistant alloy systems or composite coatings to overcome this bottleneck; Ceramic coatings achieve high hardness through their nanocrystalline structure and

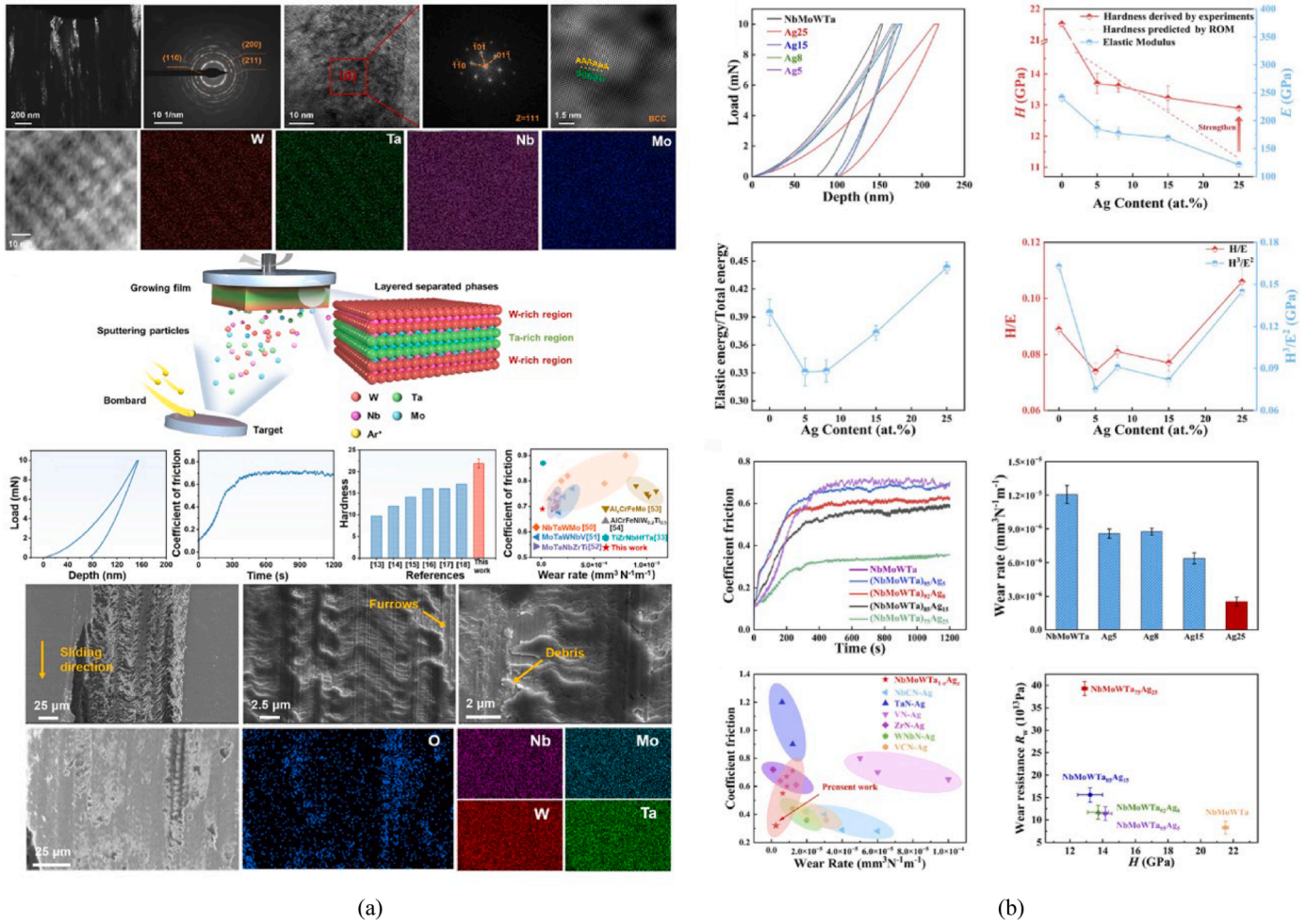

(a) (b)

Fig. 16. (a) Cross-sectional microscopic characterization of NbMoWTa films, schematic diagram of film preparation, and tribological properties [151]; (b) Mechanical and tribological properties of $(NbMoWTa)_{1-x}Ag_x$ RHEA films [152].

adaptive oxide film, but are prone to delamination and failure due to brittle aggregation and thermal mismatch. The future direction is to enhance toughness through multi-layer and nanocomposite structure design, optimize interface gradient layers to improve compatibility, and enhance stability in complex environments; DLC coatings relies on sp^3 hybrid carbon mesh to achieve ultra-low friction, but high-temperature graphitization leads to performance degradation. Future development focuses on suppressing graphitization and optimizing interface bonding through element doping to enhance durability in extreme environments; HEA coatings exhibit outstanding performance under extreme working conditions through multi principal component solid solution strengthening and in-situ self-lubricating phases, but face challenges in phase control and large-scale preparation. The core of the future lies in designing stable phase structures through compositional gradients and developing innovative sedimentation techniques for large-scale applications.

Future research of high-pressure piston pump surface coating technology needs to focus on conducting interface atomic level regulation and coating-substrate synergy optimization mechanism research, focusing on gradient component design, multi-layer structure construction and pulse laser deposition process innovation. Through precision regulation interface combining strength, residual stress distribution and phase change behavior, to achieve interface stress release and toughness synergy enhancement. It is necessary to strengthen the development of multi-functional composite coating systems, integrating wear-resistant, corrosion-resistant and self-lubricating properties to adapt to extreme environments, ultimately providing long-life, high reliability surface engineering solutions for aerospace, deep sea equipment and other fields.

CRediT authorship contribution statement

Yifei Dong: Writing – original draft, Visualization, Conceptualization. **Zhichao Jiao:** Visualization, Methodology, Investigation. **Yangyang Ma:** Visualization, Methodology, Investigation. **Qing Zhou:** Writing – review & editing, Supervision, Resources, Project administration, Methodology, Investigation, Funding acquisition, Formal analysis, Conceptualization. **Ming Yang:** Visualization, Investigation. **Xing Ran:** Writing – review & editing, Supervision, Conceptualization. **Zhe Wang:** Methodology, Data curation. **Chengjiang Tang:** Methodology, Formal analysis. **Yulong Li:** Writing – review & editing, Supervision, Investigation, Conceptualization. **Xiner Li:** Methodology, Investigation, Formal analysis. **Haishan Teng:** Investigation, Formal analysis. **Xiaojiang Lu:** Investigation, Formal analysis, Conceptualization. **Xuebo Liu:** Visualization, Methodology.

Declaration of competing interest

The authors declare that they have no known competing financial interests or personal relationships that could have appeared to influence the work reported in this paper.

Acknowledgments

The authors would like to thank the Natural Science Foundation of China (Grant No. 52471093), the Guangdong Basic and Applied Basic Research Foundation (Grant No. 2024A1515012378),the State Key Laboratory of Solidification Processing Program of China (Grant No. 2025-QZ-03).

References

[1] Zhang J, et al. Analysis of the cylinder block tilting inertia moment and its effect on the performance of high-speed electro-hydrostatic actuator pumps of aircraft. Chin J Aeronaut 2018;31(1):169–77.
[2] Ma Z, et al. Fault diagnosis of an intelligent hydraulic pump based on a nonlinear unknown input observer. Chin J Aeronaut 2018;31(2):385–94.
[3] Guo S, et al. Hydraulic piston pump in civil aircraft: current status, future directions and critical technologies. Chin J Aeronaut 2020;33(1):16–30.
[4] Tang S, et al. An improved convolutional neural network with an adaptable learning rate towards multi-signal fault diagnosis of hydraulic piston pump. Adv Eng Inform 2021;50:101406.
[5] He Y, et al. A deep multi-signal fusion adversarial model based transfer learning and residual network for axial piston pump fault diagnosis. Measurement 2022;192:110889.
[6] Boretti A. Towards hydrogen gas turbine engines aviation: a review of production, infrastructure, storage, aircraft design and combustion technologies. Int J Hydrogen Energy 2024;88:279–88.
[7] Kazama T. Application of a mixed lubrication model for hydrostatic thrust bearings of hydraulic equipment. Trans Asme J Tribol 1993;115(4):686–91.
[8] Yamaguchi A, Matsuoka H. A mixed lubrication model applicable to bearing/seal parts of hydraulic equipment. J Tribol J Tribol 1992;114(1):116–21.
[9] Pelosi M, Ivantysynova M. A geometric multigrid solver for the piston–cylinder interface of axial piston machines. Tribol Trans 2012;55(2):163–74.
[10] Xu B, et al. Investigation on structural optimization of anti-overturning slipper of axial piston pump. Sci China Technol Sci 2012;55(11):3010–8.
[11] Wang H, et al. Structural improvement, material selection and surface treatment for improved tribological performance of friction pairs in axial piston pumps: a review. Tribol Int 2024;198:109838.
[12] Wang S, et al. Minimum entropy deconvolution based on simulation-determined band pass filter to detect faults in axial piston pump bearings. ISA (Instrum Soc Am) Trans 2019;88:186–98.
[13] Fu S, et al. DCSIAN: a novel deep cross-scale interactive attention network for fault diagnosis of aviation hydraulic pumps and generalizable applications. Reliab Eng Syst Saf 2024;249:110246.
[14] Zou Q, et al. Abrasive wear model for lubricated sliding contacts. Wear 1996;196(1):72–6.
[15] Dong C, et al. Inverse transient analysis based calibration of surrogate pipeline model for fault simulation of axial piston pumps. Mech Syst Signal Process 2023;205:110829.
[16] Lyu F, et al. Research on wear prediction of piston/cylinder pair in axial piston pumps. Wear 2020:456–7.
[17] Haneef M, et al. Wear control and friction reduction in newly developed multilayer Mg-DLC coatings using organic base oil and sustainable lubrication additives. Wear 2025;572–573:206067.
[18] Tyagi A, et al. A critical review of diamond like carbon coating for wear resistance applications. Int J Refract Metals Hard Mater 2019;78:107–22.
[19] Salerno E, et al. Friction and wear characteristics of DLC-terminated coatings deposited on AlSi10Mg alloy produced by additive manufacturing. Surf Coating Technol 2024;494:131422.
[20] Arroyo A, et al. Structural modification of electrodeposited nickel coatings by ceramic particles incorporation to enhance corrosion-erosion resistance. J Mater Res Technol 2025;35:7332–45.
[21] Shi X, et al. Tribological behavior of polydopamine-modified boron nitride nanoplatelets-reinforced silicate ceramic coatings. Ceram Int 2025;51(12, Part A):16224–33.
[22] Yang Y, et al. Self-lubricating ceramic-fluoride composite coatings for seawater/atmospheric environments: evolution of microstructure, phase, mechanical, corrosion and tribological properties. Ceram Int 2025;51(13):17968–83.
[23] Jian Z, et al. Investigation of wear behavior of graphite coating on aluminum piston skirt of automobile engine. Eng Fail Anal 2019;97:408–15.
[24] Xie Y, et al. Superior tribocorrosion resistance of Mg metal matrix composite by self-sealing PEO coating. Corros Sci 2025;251:112938.
[25] Habib KA, et al. Systematic approach to paired ceramic coatings deposited by oxygen fuel and metal in a tribological application. J Mater Res Technol 2025;35:1141–56.
[26] Gao W, et al. Microstructure evolution, wear resistance and corrosion resistance of CoCrCu0.5FeNiSix high-entropy alloy coatings fabricated by laser cladding. J Mater Res Technol 2025;36:5539–58.
[27] Jia H, et al. Microstructure, wear and corrosion properties of laser melted CoCrNiFeTix high-entropy alloy coatings on copper alloys. J Alloys Compd 2025;1021:179674.
[28] Chen D, et al. Improvement of tribological properties of ion-nitrided FeCoCrNiNb gradient high-entropy alloy coatings. J Alloys Compd 2025;1020:179483.
[29] Luo F, et al. Wear behavior of single-layer graphene oxide reinforced CoCrFeNiMn HEA coating by laser cladding. Intermetallics 2024;175:108512.
[30] Guo Y, et al. Competitive relationship between the FCC + BCC dual phases in the wear mechanism of laser cladding FeCoCrNiAl0.5Ti0.5 HEAs coating. Surf Coating Technol 2024;493:131315.
[31] Zhang Z, et al. Microstructure and wear behavior of $(CoCrFeNiMn)_{1-x}/(WC)_x$ composite coatings fabricated by directed energy deposition. Wear 2025;578–579:206205.
[32] Sabarinath S, et al. High entropy alloy (HEA) coatings for tribological applications - a review. Results Eng 2025;27:105695.
[33] Tan J, et al. Soft magnetic composites insulating coating technology: a review. Mater Today Commun 2025;48:113395.
[34] Jia H, et al. A review of metal hydride coating technology: applications and challenges in energy storage and catalysis. Int J Hydrogen Energy 2025;149:150080.
[35] Abdoos M, et al. Effect of coating thickness on the tool wear performance of low stress TiAlN PVD coating during turning of compacted graphite iron (CGI). Wear 2019;422–423:128–36.
[36] Tapia-Ramírez VH, et al. Effect of nitrogen doping on the mechanical and tribological properties of hydrogen-free DLC coatings deposited by arc-PVD at an industrial scale. Surf Coating Technol 2025;499:131825.
[37] Yu S, et al. Tribological and corrosive performance of functional gradient DLC coatings prepared by a hybrid HiPIMS/CVD techniques. Vacuum 2025;238:114160.
[38] Zou J, et al. Corrosion and wear resistance improvements in NiCu alloys through flame-grown honeycomb carbon and CVD of graphene coatings. Surf Coating Technol 2023;473:130040.
[39] Selvaraj J, et al. A comparative review on cold sprayed cermet coatings and their applications in high temperature corrosion, oxidation and wear resistance. Results Surf Interfaces 2025;20:100589.
[40] Shahana M, et al. Strain induced microstructural changes in cold sprayed IN718 coating. Scr Mater 2025;266:116796.
[41] Guduru RK, et al. A critical review on thermal spray based manufacturing technologies. Mater Today Proc 2022;62:7265–9.
[42] Vignesh S, et al. Identifying the optimal HVOF spray parameters to attain minimum porosity and maximum hardness in iron based amorphous metallic coatings. Def Technol 2017;13(2):101–10.
[43] Wang L, et al. Improving mechanical strength of vacuum brazed joints via laser texturing combined with electroplating. Mater Today Commun 2025;44:111871.
[44] Atuanya CU, et al. Experimental study on the microstructural and anti-corrosion behaviour of Co-deposition Ni–Co–SiO_2 composite coating on mild steel. Def Technol 2018;14(1):64–9.
[45] Fayomi OSI, et al. Electrolytic deposition of super-smart composite coating of Zn-V_2O_5-NbO_2 on low carbon steel for defence application. Def Technol 2018;14(5):446–50.
[46] Flott LW. Metal finishing: an overview. Met Finish 2002;100(1):16–30.
[47] Wan S, et al. Microstructure and properties of cold sprayed aluminum bronze coating on MBLS10A-200 magnesium-lithium alloy. Mater Chem Phys 2022;281:125832.
[48] Das P, et al. Tribological behaviour of HVOF sprayed diamond reinforced bronze coatings. Diam Relat Mater 2019;93:16–25.
[49] D'Andrea D, et al. Failure analysis of anti-friction coating for cylinder blocks in axial piston pumps. Eng Fail Anal 2019;104:126–38.
[50] Shang X, et al. Structural modulation and fretting wear performance of Ag-Fe_2O_3 nanocomposite coating constructed using friction loading: impact of soft-hard phase deposition sequence. Mater Today Commun 2025:112789.
[51] Zhang G, et al. Superior self-lubricating coatings with heterogeneous nanocomposite structures on ti-nb-zr-ta-hf refractory multi-principal element alloy. Adv Funct Mater 2024;34(44):2405657.
[52] Das P, et al. HVOF sprayed diamond reinforced nano-structured bronze coatings. J Alloys Compd 2018;746:361–9.
[53] Liang W, et al. Microstructures and properties of PVD aluminum bronze coatings. Thin Solid Films 2000;376(1):159–63.
[54] Marathe I, et al. Electrodeposition of multi component alloys for hydrogen evolution reaction – a review. Next Mater 2025;9:101023.
[55] Radhika N, et al. Machine learning insights for predicting density and hardness in centrifugal SHS synthesized ceramic coatings. Results Eng 2025:27:106682.
[56] N R, et al. A comparative analysis of machine learning techniques for predicting the wear rate of ceramic coated steel. IEEE Access 2024;12:146949–67.
[57] Li CJ, et al. The bonding formation during thermal spraying of ceramic

coatings: a review. J Therm Spray Technol 2022;31(4):780–817.
[58] Hassanin H, et al. Micro-fabrication of ceramics: additive manufacturing and conventional technologies. J Adv Ceram 2021;10(1):1–27.
[59] Mehta A, Vasudev H. Advancements in ceramic-coated metals: enhancing thermal spray coatings for improved performance in aerospace applications using surface treatments. Results Surf Interfaces 2025;18:100387.
[60] Zhang Z, et al. High temperature sand erosion failure mechanism of ceramic/metal multilayer coating. Ceram Int 2025;51(2):2398–410.
[61] Siengchin S. A review on lightweight materials for defence applications: present and future developments. Def Technol 2023;24:1–17.
[62] Sun W, et al. The influence of metal element types on the formation mechanism and properties of high-entropy ceramic powders and coatings. J Alloys Compd 2025;1010:177680.
[63] Ötken ÖF, et al. High-temperature aqueous corrosion of MO–Na_2O–B_2O_3–SiO_2 glass and glass-ceramic coatings on metallic substrates: Effect of alkaline earth metals M^{2+}= {Ca^{2+}, Sr^{2+}, Ba^{2+}. J Eur Ceram Soc 2025;45(1):116820.
[64] Khadem M, et al. Tribology of multilayer coatings for wear reduction: a review. Friction 2017;5(3):248–62.
[65] Liu J, et al. Research and development status of laser cladding on magnesium alloys: a review. Opt Laser Eng 2017;93:195–210.
[66] Diao Y, Zhang K. Microstructure and corrosion resistance of TC2 Ti alloy by laser cladding with Ti/TiC/TiB2 powders. Appl Surf Sci 2015;352:163–8.
[67] Sexton L, et al. Laser cladding of aerospace materials. J Mater Process Technol 2002;122(1):63–8.
[68] Sui X, et al. Effect of specific energy on microstructure and properties of laser cladded TiN/Ti3AlN-Ti3Al composite coating. Opt Laser Technol 2020;131:106428.
[69] Pan X, et al. Superior wear resistance in cast aluminum alloy via femtosecond laser induced periodic surface structures and surface hardening layer. Appl Surf Sci 2023;636:157866.
[70] Lin H, et al. Optimization for enhancing resistance to brittle fracture using the phase field model integrating strain gradient. Comput Methods Appl Mech Eng 2025;446:118278.
[71] Xia Q, et al. Unveiling the dislocation mechanism induced by irradiation defects in austenitic FeCrNi alloy. Int J Plast 2025;193:104451.
[72] Zhou Y, et al. Predicting intergranular stress corrosion cracking of stainless steels in high-temperature water by incorporating crystallographic factor. Acta Mater 2025;297:121322.
[73] Konstantiniuk F, et al. Annealing activated substrate element diffusion and its influence on the microstructure and mechanical properties of CVD TiN/TiCN coatings. Surf Coating Technol 2024;488:131079.
[74] Hao J, et al. Effects of interface configurations on strengthening-toughening and tribological behaviors of TiC/Ti nano-multilayers. Surf Coating Technol 2025;497:131726.
[75] Maksakova O, et al. Tribological and micromechanical performance of hard yet tough TiSiN/WN coatings: an experimental analysis of multilayer effects. Int J Refract Metals Hard Mater 2025;131:107212.
[76] Wu M, et al. Influence of bilayer period and thickness ratio on the mechanical and tribological properties of CrSiN/TiAlN multilayer coatings. Surf Coating Technol 2011;206(7):1886–92.
[77] Zhang H, et al. Evolution and mechanism of frictional properties of DLC coatings and iron surfaces under hydrogen-atom irradiation. Carbon 2025;244:120658.
[78] Androulidakis C, et al. Tunable macroscale structural superlubricity in two-layer graphene via strain engineering. Nat Commun 2020;11(1).
[79] Price MR, Raeymaekers B. Quantifying adhesion of ultra-thin multi-layer DLC coatings to Ni and Si substrates using shear, tension, and nanoscratch molecular dynamics simulations. Acta Mater 2017;141:317–26.
[80] Robertson J. Diamond-like amorphous carbon. Mater Sci Eng R Rep 2002;37(4):129–281.
[81] Grill A. Diamond-like carbon: state of the art. Diam Relat Mater 1999;8(2):428–34.
[82] Shi Y, et al. Insights into irradiation-affected structural evolution and mechanical behavior of amorphous carbon. Acta Mater 2024;281:120424.
[83] Artini C, Muolo ML, Passerone A. Diamond–metal interfaces in cutting tools: a review. J Mater Sci 2012;47(7):3252–64.
[84] Nisar A, et al. Oxidation studies on TaC based ultra-high temperature ceramic composites under plasma arc jet exposure. Corros Sci 2016;109:50–61.
[85] Jiang J, et al. Preparation and properties of C/TaC composites via PIP process. Ceram Int 2017;43(2):2379–83.
[86] Liu G, et al. Atomic oxygen damage behavior of TaC coating-modified C/C composite. J Eur Ceram Soc 2020;40(3):642–50.
[87] Kong JA, et al. Influence of crystallite morphology on the ablative behaviors of CVD-TaC coatings prepared on C/C composites beyond 2100 °C. Corros Sci 2022;205:110426.
[88] Martyanov A, et al. Microcrystalline and nanocrystalline structure of diamond films grown by MPCVD with nitrogen additions: study of transitional synthesis conditions. J Cryst Growth 2024;648:127916.
[89] Goti E, et al. The tribological performance of super-hard Ta:C DLC coatings obtained by low-temperature PVD. Ceram Int 2023;49(24, Part A):40193–210.
[90] Erdemir A, Martin JM. Superior wear resistance of diamond and DLC coatings. Curr Opin Solid State Mater Sci 2018;22(6):243–54.
[91] Efeoglu I, et al. Adhesion and friction-wear characterization of W-doped hydrogenated diamond-like carbon (a-C:H) coatings. Surf Coating Technol 2025;495:131578.
[92] Wang J, et al. Tuning of the microstructure, mechanical and tribological properties of a-C:H films by bias voltage of high frequency unipolar pulse. Appl Surf Sci 2015;356:695–700.
[93] Zur IA, et al. Influence of humidity on the electrophysical properties and charge transfer mechanism in nanoscale diamond-like carbon coatings. Carbon 2025;237:120100.
[94] Jiao Z, et al. Enhancing tribocorrosion resistance of VCoNi alloys in artificial seawater via nitrogen alloying. Corros Sci 2025;243:112600.
[95] Jiao Z, et al. Self-generating hierarchical lubricious phase for superior high-temperature tribological performance in multi-principal element alloys. Scr Mater 2025;268:116843.
[96] Ye W, et al. Superior wear performance of CoCrNi matrix composite reinforced with quasi-continuously networked graphene nanosheets and in-situ carbide. Friction 2025;13(8):9441001.
[97] Zou Y, et al. Nanocrystalline high-entropy alloys: a new paradigm in high-temperature strength and stability. Nano Lett 2017;17(3):1569–74.
[98] Lou B, et al. Exploring the effect of Ti and Al contents on the microstructural, mechanical, and corrosion resistance features of VNbMoTaWTiAlN refractory high entropy alloy coatings. Mater Chem Phys 2025;341:130901.
[99] Jiani H, et al. Heterostructured multi-principal element alloys prepared by laser-based techniques. Microstructures 2025;5(2):2025021.
[100] Tao Y, et al. Improved high-temperature oxidation resistance and enhancement mechanism of laser deposited NiCoFeCrxSiAlCu0.5TiMoB0.4 high-entropy alloy coatings by Cr doping. J Alloys Compd 2025;1026:180375.
[101] Hu J, et al. Laser-clad AlNbTiVZr lightweight refractory high-entropy alloy coating on Ti_6Al_4V: microstructural characterization and wear resistance. J Alloys Compd 2025;1026:180425.
[102] Yeh J. Alloy design strategies and future trends in high-entropy alloys. J Occup Med 2013;65(12):1759–71.
[103] Luo D, et al. Design and characterization of self-lubricating refractory high entropy alloy-based multilayered films. ACS Appl Mater Interfaces 2021;13(46):55712–25.
[104] Zhao J, et al. Review of cylinder block/valve plate interface in axial piston pumps: theoretical models, experimental investigations, and optimal design. Chin J Aeronaut 2021;34(1):111–34.
[105] Hao W, et al. A comparative investigation on wear behaviors of physical and chemical vapor deposited bronze coatings for hydraulic piston pump. Chin J Aeronaut 2024;37(3):391–403.
[106] Guo X, et al. Microstructure, microhardness and dry friction behavior of cold-sprayed tin bronze coatings. Appl Surf Sci 2007;254(5):1482–8.
[107] Yin TY, et al. Effect of laser energy density on microstructural evolution and wear resistance of modified aluminum bronze coatings fabricated by laser cladding. Mater Chem Phys 2022;285:126191.
[108] Miguel JM, et al. Effect of the spraying process on the microstructure and tribological properties of bronze–alumina composite coatings. Surf Coating Technol 2010;205(7):2184–90.
[109] Miguel JM, et al. Tribological behavior of bronze composite coatings obtained by plasma thermal spraying. Tribol Lett 2011;42(3):263–73.
[110] Chen TK, et al. Nanostructured nitride films of multi-element high-entropy alloys by reactive DC sputtering. Surf Coating Technol 2004;188–189:193–200.
[111] Ashvita AJ, et al. Comparative study on surface modification of heat-treated hot work tool steel using plasma nitriding and thin film deposition technique. Mater Today Proc 2024. https://doi.org/10.1016/j.matpr.2024.05.11.
[112] Jafarpour SM, et al. Solid carbon active screen plasma nitrocarburizing of AISI 316L stainless steel in cold wall reactor: influence of plasma conditions. J Mater Res Technol 2020;9(4):9195–205.
[113] Schramm A, et al. Effect of bias plasma on active screen nitrocarburising response of AISI 420 martensitic stainless steel. Vacuum 2022;205:111389.
[114] Khanzadeh M, et al. The influence of carbon and nitrogen doping on the electrical, mechanical, thermodynamic, and hydrogen dissolution properties of zirconium-based ceramics: a comprehensive study. Ceram Int 2025;51(7):8855–70.
[115] Cui Z, An J. Growth mechanisms and properties of carburized layers with a certain extent of surface oxidation on TA1 and TC21 alloys during the process of conventional solid pack carburizing. J Mater Res Technol 2025;38:1457–71.
[116] Zhang H, et al. The energetic, electronic and mechanical properties of metal (Fe/Co/Ni/Cu) || ceramics (TiN) interfaces: a first-principles study. Mater Today Commun 2025;42:111281.
[117] Lapitskaya V, et al. Microstructure and properties of thin AlN coatings with different stoichiometric compositions. Mater Res Bull 2025;187:113380.
[118] Xu K, et al. Optical optimization and thermal stability of SiN/Ag/SiN based transparent heat reflecting coatings. Infrared Phys Technol 2022;122:104089.
[119] Hu H, et al. Enhancing the wear resistance of AISI 201 alloy by the addition of TiN particles through ultrasonic shot peening. Vacuum 2025;236:114180.
[120] Hong Y, et al. Improvement of the low-speed friction characteristics of a hydraulic piston pump by PVD-coating of TiN. J Mech Sci Technol 2006;20(3):358–65.
[121] Lee SY, et al. Application of the duplex TiN coatings to improve the

tribological properties of electro hydrostatic Actuator pump parts. Surf Coating Technol 2005;193(1):266–71.
[122] Shakib SE, et al. Nanomechanical assessment of tribological behavior of TiN/TiCN multi-layer hard coatings deposited by physical vapor deposition. J Mater Res Technol 2023;25:1344–54.
[123] He Z, et al. Effect of heat-treatment of Ti/graphite powders on the microstructure and mechanical properties of reactive plasma sprayed TiCN coatings. Diam Relat Mater 2022;129:109301.
[124] Özkan D, et al. Wear and friction behavior of CrTiN/TiCN and CrTiN/CrCN multilayer composite coatings. Ceram Int 2022;48(10):13732–47.
[125] Kaosar Saad Safin, et al. Application of PVD coatings in medical implantology for enhanced performance, biocompatibility, and quality of life. Heliyon 2024;10(16):e35541.
[126] Peng D, et al. Sliding friction behaviors of TiCN/Cr_3C_2-NiCr and TiCN/WC-CoCr duplex coatings fabricated by combining HVOF and HT-CVD procedures. Surf Coating Technol 2023;474:130078.
[127] Lee S, Hong Y. Effect of CrSiN thin film coating on the improvement of the low-speed torque efficiency of a hydraulic piston pump. Surf Coating Technol 2007;202(4):1129–34.
[128] Lee SY, et al. Effect of Si doping on the wear properties of CrN coatings synthesized by unbalanced magnetron sputtering. Thin Solid Films 2006;506–507:192–6.
[129] Kim G, et al. Structure and mechanical properties of Cr–Zr–N films synthesized by closed field unbalanced magnetron sputtering with vertical magnetron sources. Surf Coating Technol 2005;200(5):1669–75.
[130] Hong Y, Lee S. A comparative study of Cr–X–N (X=Zr, Si) coatings for the improvement of the low-speed torque efficiency of a hydraulic piston pump. Met Mater Int 2008;14(1):33–40.
[131] Rosso M, et al. Corrosion resistance and properties of pump pistons coated with hard materials. Int J Refract Metals Hard Mater 2001;19(1):45–52.
[132] Aktarer SM. Tribological properties under dry and lubricated sliding conditions of TiSiN and AlTiCrN coatings deposited on gray cast iron. Surf Interfaces 2024;52:104948.
[133] Schuhler G, et al. Wear mechanisms in contacts involving slippers in axial piston pumps: a multi-technical analysis. J Mater Eng Perform 2018;27(10):5395–405.
[134] Hong Y, et al. Application of a DLC-Coating for improving hydrostatic piston shoe bearing performance under mixed friction conditions. Int J Precis Eng Manuf 2015;16(2):335–41.
[135] Kalin M, et al. Analyses of the long-term performance and tribological behavior of an axial piston pump using Diamondlike-Carbon-Coated piston shoes and biodegradable oil. J Tribol ASME 2008:130.
[136] Schuhler G, et al. Efficacy of coatings and thermochemical treatments to improve wear resistance of axial piston pumps. Tribol Int 2018;126:376–85.
[137] Manhabosco TM, et al. Corrosion, wear and wear–corrosion behavior of graphite-like a-C:H films deposited on bare and nitrided titanium alloy. Diam Relat Mater 2013;31:58–64.
[138] Dalibón EL, et al. Soft and thick DLC deposited on AISI 316L stainless steel with nitriding as pre-treatment tested in severe wear conditions. Diam Relat Mater 2020;106:107881.
[139] Dalibón EL, et al. Mechanical and corrosion behavior of thick and soft DLC coatings. Surf Coating Technol 2017;312:101–9.
[140] Zhou Y, et al. Tribological performance of hydrogenated diamond-like carbon coating deposited on superelastic 60NiTi alloy for aviation self-lubricating spherical plain bearings. Chin J Aeronaut 2022;35(12):309–20.
[141] Khanlari K, et al. Reciprocating sliding wear behavior of 60NiTi As compared to 440C steel under lubricated and unlubricated conditions. Tribol Trans 2018;61(6):991–1002.
[142] Ma P, et al. Enhanced mechanical and electrochemical performance of CoCrNi medium entropy alloy through multi-scale heterostructure. Vacuum 2025;238:114267.
[143] Chen Z, et al. Microstructure evolution and wear behavior at room and high temperatures of Mo2C particle reinforced CoCrFeNiMn high-entropy alloys composite coatings prepared by induction cladding. Surf Coating Technol 2025;503:132001.
[144] Wang Y, et al. Investigation on the wear performance of CoCrNi matrix self-lubricating composites at cryogenic temperature. Surf Coating Technol 2025;500:131906.
[145] Aliyu A, Srivastava C. Phase constitution, surface chemistry and corrosion behavior of electrodeposited MnFeCoNiCu high entropy alloy-graphene oxide composite coatings. Surf Coating Technol 2022;429:127943.
[146] Gu J, et al. Microstructure and wear resistance of multi-layer graphene doped AlCoCrFeNi2.1 high-entropy alloy self-lubricating coating prepared by laser cladding. Intermetallics 2025;176:108578.
[147] Zhang D, et al. Effect of graphene oxide on CoCrFeNi high-entropy alloy coatings prepared by the electrodeposition method. Surf Coating Technol 2024;485:130919.
[148] Liu C, et al. Preparation of graphene/AlCoCrNiTiMox coatings by laser parameter optimization based on TRIZ theory and its application in extending the service life of surveying and mapping drones. Mater Today Commun 2024;41:110537.
[149] Li S, et al. The deformation mechanism of graphene nanosheets embedded in high-entropy alloy upon sliding. Carbon 2024;229:119532.
[150] Hua D, et al. Atomistic insights into the role of graphene sheets in CoCrNi/graphene composites. Acta Mater 2025;287:120809.
[151] Jiao Z, et al. Super-hard refractory high entropy alloy film with spinodal decomposition. J Mater Sci Technol 2025;213:190–5.
[152] Zhou Q, et al. Microstructure, mechanical and tribological properties of NbMoWTaAg refractory high entropy films with nano-layered self-organization. Tribol Int 2024;198:109888.